

ROBUSTLY IDENTIFYING CONCEPTS INTRODUCED DURING CHAT FINE-TUNING USING CROSSCODERS

Content Warning: This paper contains examples of harmful language

Julian Minder^{*, $\text{\textcircled{a}}$, $\text{\textcircled{a}}$} Clément Dumas^{*, \textdagger , \textdagger}
Caden Juang ^{$\text{\textcircled{d}}$} Bilal Chughtai Neel Nanda
 ^{$\text{\textcircled{a}}$} EPFL ^{$\text{\textcircled{e}}$} ETHZ ^{\textdagger} Ecole Normale Supérieure Paris-Saclay ^{\textdagger} Université Paris-Saclay
 ^{$\text{\textcircled{d}}$} Northeastern University
julian.minder@epfl.ch, clement.dumas@ens-paris-saclay.fr

ABSTRACT

Model diffing is the study of how fine-tuning changes a model’s representations and internal algorithms. Many behaviours of interest are introduced during fine-tuning, and model diffing offers a promising lens to interpret such behaviors. Crosscoders (Lindsey et al., 2024) are a recent model diffing method that learns a shared dictionary of interpretable concepts represented as latent directions in both the base and fine-tuned models, allowing us to track how concepts shift or emerge during fine-tuning. Notably, prior work has observed concepts with no direction in the base model, and it was hypothesized that these model-specific latents were concepts introduced during fine-tuning. However, we identify two issues which stem from the crosscoders L1 training loss that can misattribute concepts as unique to the fine-tuned model, when they really exist in both models. We develop Latent Scaling to flag these issues by more accurately measuring each latent’s presence across models. In experiments comparing Gemma 2 2B base and chat models, we observe that the standard crosscoder suffers heavily from these issues. Building on these insights, we train a crosscoder with BatchTopK loss (Bussmann et al., 2024) and show that it substantially mitigates these issues, finding more genuinely chat-specific and highly interpretable concepts. We recommend practitioners adopt similar techniques. Using the BatchTopK crosscoder, we successfully identify a set of genuinely chat-specific latents that are both interpretable and causally effective, representing concepts such as *false information* and *personal question*, along with multiple refusal-related latents that show nuanced preferences for different refusal triggers. Overall, our work advances best practices for the crosscoder-based methodology for model diffing and demonstrates that it can provide concrete insights into how chat tuning modifies language model behavior.¹

*Equal contribution. Order randomized.

¹We open-source our models and data at <https://huggingface.co/science-of-finetuning>. Our library to train crosscoders is available at https://github.com/jkminder/dictionary_learning. The code to reproduce our results will be released at a later date.

1 INTRODUCTION

Classically, the goal of mechanistic interpretability (Sharkey et al., 2025; Mueller et al., 2024; Ferrando et al., 2024; Elhage et al., 2021; Olah et al., 2020) research has been to understand either an entire model (Huben et al., 2024; Elhage et al., 2022), or to understand specific *circuits*, or algorithms, that are implemented by the model to solve particular tasks (Wang et al., 2023a). This is akin to trying to understand the entire source code of a running computer program, and is challenging. *Model diffing* is a relatively nascent approach that instead attempts to detect what has *changed* in a model as a result of fine-tuning. Given the relatively small compute used for present-day fine-tuning compared to pre-training, we expect the changes introduced to be limited in scope – perhaps akin to a pull request on a large code repository.

Pretraining teaches the model general world knowledge, generic circuitry and skills. These are broadly useful in a variety of settings. Fine-tuning has little reason to change most of this cognition. It seems likely the fine-tuned model will share many representations with the base model, and only specific aspects will change. For instance, the model’s persona, chat specific skills that help it follow instructions and reply to users, and other task specific skills more broadly. This argument suggests that the model diffing approach to mechanistic interpretability might be comparatively *easier* than trying to understand the full model.

Model diffing might also be incredibly useful. The process of fine-tuning a model is what makes it *useful* as a tool or agent. Better understanding the mechanisms that give reasoning models (DeepSeek-AI et al., 2025; OpenAI et al., 2024) heightened capabilities as compared to base or chat models might allow us to debug their failures and improve them. Fine-tuning also often introduces a number of problematic behaviors, for example, sycophancy (Sharma et al., 2023). Future AI safety and alignment concerns (Greenblatt et al., 2024; Meinke et al., 2025) may emerge specifically in fine-tuned models. For example, long-horizon RL could incentivize models to exploit reward signals and act deceptively, building on deception concepts already learned during pretraining. It’s possible model diffing will be sufficient to allow us to detect this.

Prior model diffing research has investigated how models change during fine-tuning (Lindsey et al., 2024; Bricken et al., 2024; Prakash et al., 2024; Lee et al., 2024; Jain et al., 2024; Khayatan et al., 2025; Thasarathan et al., 2025; Wu et al., 2024; Mosbach, 2023; Merchant et al., 2020; Hao et al., 2020; Kovaleva et al., 2019). While these studies have hypothesized that fine-tuning primarily shifts and repurposes existing capabilities rather than developing entirely new ones, conclusive evidence for this claim remains elusive. Model diffing remains a nascent field that lacks established consensus and mature analytical tools. Much prior work has leveraged ad-hoc techniques for understanding how models change in narrow ways (e.g. studying how a particular circuit, algorithm, or representation changes) (Prakash et al., 2024; Lee et al., 2024; Wu et al., 2024; Hao et al., 2020; Kovaleva et al., 2019), or have been on toy models (Jain et al., 2024; Minder, 2024). It is unclear whether many prior approaches would scale to understanding the kinds of fine-tuning large models actually undergo.

Recently, Lindsey et al. (2024) introduced a new tool for model diffing, the **crosscoder**, which may overcome the issues discussed above. Crosscoders build on the popular sparse autoencoder (SAE) (Huben et al., 2024; Bricken et al., 2023; Yun et al., 2021), which has shown promise for interpreting a model’s representations by decomposing activations into a sum of sparsely activating dictionary elements. There are many variants of crosscoders; the variant we are concerned with in this paper concatenates the activations of the base and fine-tuned model residual streams and trains a shared dictionary across this activation stack. Thus, for each dictionary element (aka "latent", corresponding to one concept), the crosscoder learns a pair of latent directions - one corresponding to the base model and one to the fine-tuned model. Crosscoders can thus potentially identify which latents are novel to the fine-tuned model, which are novel to the base-model, and which are shared.

We term these sets chat-only, base-only, and shared respectively. Lindsey et al. (2024) identify chat-only latents by looking at the norm of the latent directions – if the latent direction of the base model has zero norm, this indicates that the latent is chat-only.

In this work, we build directly on Lindsey et al. (2024). We critically examine the crosscoder, and its efficacy for model diffing. Our contributions are as follows:

1. We identify two theoretical limitations of the crosscoder training objective, that may lead to falsely identified chat-only latents (Section 2.3).
 - (a) Complete Shrinkage: The sparsity loss can force base latent directions to zero norm, even when they contribute to base model reconstruction, particularly when a latent is more important for the chat model but still relevant for the base model.
 - (b) Latent Decoupling: The crosscoder may represent a shared concept using a chat-only latent when it is actually encoded by a different combination of latents in the base model, as the crosscoder’s sparsity loss treats both representations as equivalent.
2. We develop an approach called *Latent Scaling* to detect spurious chat-only latents, inspired by Wright & Sharkey (2024) (Section 2.3.3). Using this approach, we demonstrate that the above issues occur in practice. While the norm-based metric from Lindsey et al. (2024) appears to identify a clean trimodal distribution of base-only, chat-only and shared latents, we show that this is an artifact of the crosscoder loss function rather than a meaningful distinction. Our conclusion is that the crosscoder loss does not actually have an inductive bias that helps to learn better model-only latents.
3. Nonetheless, we demonstrate that crosscoders trained with BatchTopK loss (Bussmann et al., 2024) exhibit robustness to the above issues (Section 3.1.1) and identify a larger number of genuine model-specific latents.
4. We show that in the BatchTopK crosscoder, the norm-based metric successfully identifies causally relevant latents by measuring their ability to reduce the prediction gap between base and chat model. In contrast, this metric fails in the L1 crosscoder, where Latent Scaling becomes necessary to identify the truly causally relevant latents. Importantly, when utilizing all available latents, both crosscoders bridge approximately the same portion of the prediction gap, suggesting they capture equivalent information despite organizing it differently.
5. We outline that the chat-only latents found by the BatchTopK crosscoder are highly interpretable (Section 3.1.3), revealing key aspects of chat model behavior such as the role of chat template tokens, persona-related questions, detection of false information, and various refusal related mechanisms.

Overall, we show that using BatchTopK loss overcomes the described limitations of L1-trained crosscoders, validating them as a useful tool for understanding fine-tuning effects in large language models.

2 METHODS

2.1 CROSSCODER ARCHITECTURES

We consider a crosscoder architecture (Lindsey et al., 2024) with two separate encoders and decoders, one corresponding to the base model and one to the chat model. We describe both the original L1 crosscoder from (Lindsey et al., 2024) as well as a BatchTopK (Bussmann et al., 2024) variant.

L1 crosscoder. Let x be an input string and $\mathbf{h}^{\text{base}}(x), \mathbf{h}^{\text{chat}}(x) \in \mathbb{R}^d$ denote the activations at a given layer at the last token of x . For a dictionary of size D , the latent activation of the j^{th} latent $f_j(x), j \in \mathcal{J} = \{1, \dots, D\}$ is computed as

$$f_j(x) = \text{ReLU}(\mathbf{e}_j^{\text{base}} \mathbf{h}^{\text{base}}(x) + \mathbf{e}_j^{\text{chat}} \mathbf{h}^{\text{chat}}(x) + b_j^{\text{enc}}) \quad (1)$$

where $\mathbf{e}_j^{\text{base}}, \mathbf{e}_j^{\text{chat}} \in \mathbb{R}^d$ are the corresponding encoder vectors and $b_j^{\text{enc}} \in \mathbb{R}$ is the encoder bias. The reconstructed activations for both models are then defined as:

$$\tilde{\mathbf{h}}^{\text{base}}(x) = \sum_j f_j(x) \mathbf{d}_j^{\text{base}} + \mathbf{b}^{\text{dec,base}} \quad (2)$$

$$\tilde{\mathbf{h}}^{\text{chat}}(x) = \sum_j f_j(x) \mathbf{d}_j^{\text{chat}} + \mathbf{b}^{\text{dec,chat}} \quad (3)$$

where $\mathbf{d}_j^{\text{base}}, \mathbf{d}_j^{\text{chat}} \in \mathbb{R}^d$ are the j^{th} decoder latents and $\mathbf{b}^{\text{dec,base}}, \mathbf{b}^{\text{dec,chat}} \in \mathbb{R}^d$ are the decoder biases. We define the reconstruction errors for the base and chat models as $\boldsymbol{\varepsilon}^{\text{base}}(x) = \mathbf{h}^{\text{base}}(x) - \tilde{\mathbf{h}}^{\text{base}}(x)$ and $\boldsymbol{\varepsilon}^{\text{chat}}(x) = \mathbf{h}^{\text{chat}}(x) - \tilde{\mathbf{h}}^{\text{chat}}(x)$. The training loss for the L1 crosscoder is a modified L1 SAE objective:

$$\mathcal{L}_{\text{L1}}(x) = \frac{1}{2} \|\boldsymbol{\varepsilon}^{\text{base}}(x_i)\|_2 + \frac{1}{2} \|\boldsymbol{\varepsilon}^{\text{chat}}(x_i)\|_2 + \mu \sum_j f_j(x) (\|\mathbf{d}_j^{\text{base}}\|_2 + \|\mathbf{d}_j^{\text{chat}}\|_2) \quad (4)$$

with μ controlling the weight of the sparsity regularization term.²

BatchTopK crosscoder. Let $\mathcal{X} = \{x_1, \dots, x_n\}$ be a batch of $|\mathcal{X}| = n$ inputs. Following Bussmann et al. (2024), we compute the latent activation function differently during training and inference. Let $f_j(x_i)$ be the latent activation function as defined in Equation (1). Given the scaled latent activation function $v(x_i, j) = f_j(x_i) (\|\mathbf{d}_j^{\text{base}}\|_2 + \|\mathbf{d}_j^{\text{chat}}\|_2)$, the training latent activation function f_j^{train} is given by:

$$f_j^{\text{train}}(x_i, \mathcal{X}) = \begin{cases} f_j(x_i) & \text{if } (x_i, j) \in \text{BATCHTOPK}(k, v, \mathcal{X}, \mathcal{J}) \\ 0 & \text{otherwise} \end{cases} \quad (5)$$

where $\text{BATCHTOPK}(k, v, \mathcal{X}, \mathcal{J})$ represents the set of indices corresponding to the top $|\mathcal{X}| \cdot k$ values of the function v across all inputs $x_i \in \mathcal{X}$ and all latents $j \in \mathcal{J}$. We now redefine the reconstruction errors and the training loss for batch \mathcal{X} as follows:

$$\boldsymbol{\varepsilon}^{\text{base}}(x_i, \mathcal{X}) = \mathbf{h}^{\text{base}}(x_i) - \left(\sum_j f_j^{\text{train}}(x_i, \mathcal{X}) \mathbf{d}_j^{\text{base}} + \mathbf{b}^{\text{dec,base}} \right) \quad (6)$$

$$\boldsymbol{\varepsilon}^{\text{chat}}(x_i, \mathcal{X}) = \mathbf{h}^{\text{chat}}(x_i) - \left(\sum_j f_j^{\text{train}}(x_i, \mathcal{X}) \mathbf{d}_j^{\text{chat}} + \mathbf{b}^{\text{dec,chat}} \right) \quad (7)$$

$$\mathcal{L}_{\text{BatchTopK}}(\mathcal{X}) = \frac{1}{n} \sum_{i=1}^n \frac{1}{2} \|\boldsymbol{\varepsilon}^{\text{base}}(x_i, \mathcal{X})\|_2 + \frac{1}{2} \|\boldsymbol{\varepsilon}^{\text{chat}}(x_i, \mathcal{X})\|_2 + \alpha \mathcal{L}_{\text{aux}}(x_i, \mathcal{X}) \quad (8)$$

²While similar to training an SAE on concatenated activations, the crosscoder’s sparsity loss uniquely promotes decoder norm differences (see Appendix A.1).

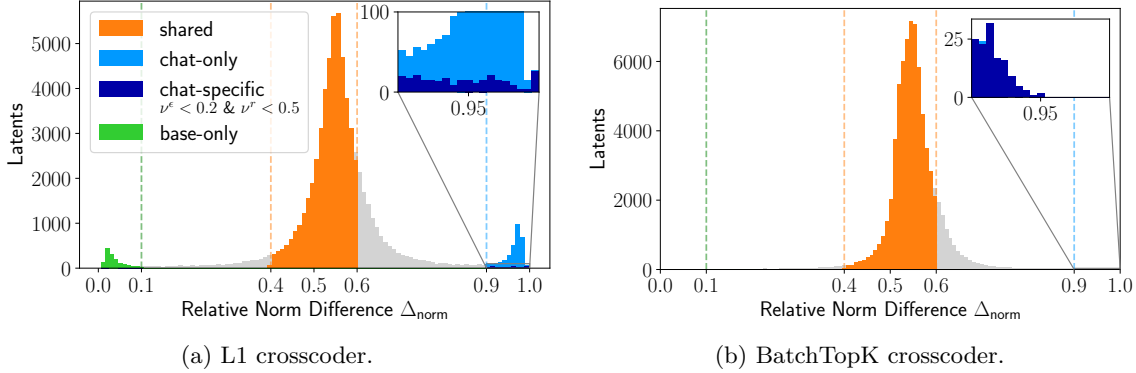


Figure 1: Histogram of decoder latent relative norm differences (Δ_{norm}) between base and chat Gemma 2 2B models (Riviere et al., 2024), as in (Lindsey et al., 2024), for both the L1 crosscoder (left) and the BatchTopK crosscoder (right). For a given latent, a value of 1 means the decoder vector for the base model is zero, indicating the latent is not useful for the base model (*chat-only* latents). Conversely, a value of 0 means the chat model’s decoder vector has a norm of zero (*base-only* latents). Values around 0.5 indicate similar decoder norms in both models, suggesting equal utility in both models (*shared* latents). We used 0.4-0.6 as the threshold for *shared* latents per prior work. We observe larger activation norms in the chat model, which shifts our distribution rightward, revealing that the chat model amplifies the norm of representations shared with the base model. We further show for both models the *chat-only* latents that are truly chat-specific and that are not affected by Complete Shrinkage ($\nu^\varepsilon < 0.2$) and Latent Decoupling ($\nu^r < 0.5$) – the *chat-specific* latents. For the original L1 crosscoder, most of the identified *chat-only* latents suffer from these issues.

The auxiliary loss facilitates the recycling of inactive latents and is defined as $\|\varepsilon^{\text{base}}(x_i, \mathcal{X}) - \varepsilon^{\hat{\text{base}}}(x_i, \mathcal{X})\|_2 + \|\varepsilon^{\text{chat}}(x_i, \mathcal{X}) - \varepsilon^{\hat{\text{chat}}}(x_i, \mathcal{X})\|_2$, where $\varepsilon^{\hat{\text{base}}}$ and $\varepsilon^{\hat{\text{chat}}}$ represent reconstructions using only the top- k_{aux} dead latents. Typically, k_{aux} is set to 512 and α to $1/32$. For inference, we employ the following latent activation function:

$$f_j^{\text{inference}}(x_i) = \begin{cases} f_j(x_i) & \text{if } v(x_i, j) > \theta \\ 0 & \text{otherwise} \end{cases} \quad (9)$$

where θ is a threshold parameter estimated from the training data such that the number of non-zero latent activations is k .

$$\theta = \mathbb{E}_{\mathcal{X}} \left[\min_{(x_i, j) \in \mathcal{X} \times \mathcal{J}} \{v(x_i, j) \mid f_j^{\text{train}}(x_i, \mathcal{X}) > 0\} \right] \quad (10)$$

2.2 DECODER NORM BASED MODEL DIFFING

To leverage crosscoders for model diffing, Lindsey et al. (2024) posit that we can exploit a key property of the architectures described above: while latent activations $f_j(x)$ are shared between models, the decoder vectors $\mathbf{d}_j^{\text{chat}}$ and $\mathbf{d}_j^{\text{base}}$ are unique to each model. When a latent j is functionally important for both models, both $\mathbf{d}_j^{\text{chat}}$ and $\mathbf{d}_j^{\text{base}}$ will have substantial non-zero norms, as each model needs those latents for accurate reconstruction. Conversely, if a latent is unique to the chat model, the optimization will assign a significant norm to $\mathbf{d}_j^{\text{chat}}$ to minimize the reconstruction error for the chat model. Since the latent is not used by the base model, the optimization will drive $\|\mathbf{d}_j^{\text{base}}\|_2$

toward zero, since this feature does not help to reconstruct the activations of the base model. Such a latent would be a *chat-only* latent.

We therefore compute the relative difference of decoder latent norms (Lindsey et al., 2024) between the base and chat models. For a latent j , the relative norm difference, Δ_{norm} , is given by

$$\Delta_{\text{norm}}(j) = \frac{1}{2} \left(\frac{\|\mathbf{d}_j^{\text{chat}}\|_2 - \|\mathbf{d}_j^{\text{base}}\|_2}{\max(\|\mathbf{d}_j^{\text{chat}}\|_2, \|\mathbf{d}_j^{\text{base}}\|_2)} + 1 \right) \quad (11)$$

This metric enables classification of latents based on their model specificity, as empirically shown in Figure 1. In practice, we classify latents into three sets based on ranges of their Δ_{norm} values: *base-only*, *chat-only* and *shared* (Table 1).

2.3 ARE *CHAT-ONLY* LATENTS REALLY CHAT-SPECIFIC?

We noted in Section 2.2 that if a latent only contributes to one model, the norm of the decoder must tend to zero for the other model. But is the converse true? Specifically, in this section we ask the question: if a latent has decoder norm zero in the base model, is it necessarily chat-specific? We focus on this set, as this is the most interesting of the three categories described in Section 2.2.

2.3.1 REASONS TO DOUBT *CHAT-ONLY* LATENTS

There are reasons to suspect *chat-only* latents might not be chat-specific. Firstly, both qualitative and quantitative analysis of L1 crosscoder latents reveals a relatively low percentage of interpretable latents within the *chat-only* set (See Section 3.1.3). More worryingly, inspection of the L1 crosscoder loss (Equation (4)) uncovers two theoretical issues that could result in latents j , which are defined by their decoder vectors \mathbf{d}_j and activation function f_j , being classified as *chat-only*, despite their presence in the activations of the base model:

Complete Shrinkage. The L1 regularization term may force the norm of the base decoder vector $\mathbf{d}_j^{\text{base}}$ to be zero, even though it is present in the base activation and could have contributed to the reconstruction of base activation. This may especially be relevant if the contribution of latent j is non-zero in the base model, but much smaller than the contribution in the chat model. Consequently, the error ϵ^{base} contains information that can be attributed to latent j .

Latent Decoupling. Latent j ‘appears’ in base activations across a subset of its latent activations but is instead reconstructed by other base decoder latents. On this subset, the base reconstruction $\tilde{\mathbf{h}}^{\text{base}}$ contains information that could be attributed to latent j . To spell this out in more detail, consider the following set up: a concept C may be represented identically in both models by some direction \mathbf{d}_C but activate on different non-exclusive data subsets. Let $f_C^{\text{chat}}(x)$ and $f_C^{\text{base}}(x)$ be concept C ’s optimal activation functions in chat and base models, defined as $f_C^{\text{chat}}(x) = f_{\text{shared}}(x) + f_{\text{c-excl}}(x)$ and $f_C^{\text{base}}(x) = f_{\text{shared}}(x) + f_{\text{b-excl}}(x)$, where f_{shared} encodes shared activation, while $f_{\text{b-excl}}$ and $f_{\text{c-excl}}$ define model exclusive activations. For interpretability, the crosscoder should ideally learn three latents:

1. A *shared* latent j_{shared} representing C when active in both models using $f_{j_{\text{shared}}} = f_{\text{shared}}$ and $\mathbf{d}_{\text{chat}} = \mathbf{d}_{\text{base}} = \mathbf{d}_C$,
2. A *chat-only* latent j_{chat} representing C when exclusively active in the chat model using $f_{j_{\text{chat}}} = f_{\text{c-excl}}$ and $\mathbf{d}_{\text{chat}} = \mathbf{d}_C$, $\mathbf{d}_{\text{base}} = \mathbf{0}$, and
3. A *base-only* latent j_{base} representing C when exclusively active in the base model using $f_{j_{\text{base}}} = f_{\text{b-excl}}$ and $\mathbf{d}_{\text{chat}} = \mathbf{0}$, $\mathbf{d}_{\text{base}} = \mathbf{d}_C$.

However, the L1 crosscoder achieves equivalent loss using just two latents:

1. A *chat-only* latent j_{chat} representing C in the chat model using $f_{j_{\text{chat}}} = f_{\text{c-excl}} + f_{\text{shared}}$ and $\mathbf{d}_{\text{chat}} = \mathbf{d}_C, \mathbf{d}_{\text{base}} = \mathbf{0}$, and
2. A *base-only* latent j_{base} representing C in the base model using $f_{j_{\text{base}}} = f_{\text{b-excl}} + f_{\text{shared}}$ and $\mathbf{d}_{\text{chat}} = \mathbf{0}, \mathbf{d}_{\text{base}} = \mathbf{d}_C$. In this scenario, the so-called “*chat-only*” latent is only truly chat-only on a subset of its activation pattern.

Although whenever $f_{\text{shared}} > 0$ two latents are active instead of one, the sparsity loss is the same because the sparsity loss includes the decoder vector norms.³

2.3.2 WHY BATCHTOPK CROSSCODERS MIGHT FIX THIS.

The BatchTopK crosscoder may address both Complete Shrinkage and Latent Decoupling issues that affect the L1 crosscoder. The key difference lies in their respective loss functions and optimization objectives.

For the L1 crosscoder, the loss function in Equation (4) includes an L1 regularization term that directly penalizes the norm of decoder vectors. This creates pressure to shrink decoder norms toward zero when a latent’s contribution is minimal, potentially causing Complete Shrinkage even when the latent has some explanatory power. In contrast, the BatchTopK crosscoder uses a different sparsity mechanism. Rather than penalizing all decoder norms, it selects only the top k most active latents per sample during training. This approach has two important advantages:

1. **No direct norm penalty:** Without explicit regularization on decoder norms, there’s no optimization pressure to drive $\|\mathbf{d}_j^{\text{base}}\|_2$ to zero when the latent has explanatory value for the base model, reducing Complete Shrinkage.
2. **Competition between latents:** The top- k selection creates competition among latents, discouraging redundant representations. This helps prevent Latent Decoupling by making it inefficient to maintain duplicate latents that encode the same information.

The BatchTopK approach thus creates an inductive bias toward learning more genuinely distinct latents, as the model must efficiently allocate its limited "budget" of k active latents per sample. This should result in fewer falsely identified *chat-only* latents and a cleaner separation between truly model-specific and shared features. Moreover, the BatchTopK crosscoder actively encourages the three-latent solution presented in the Latent Decoupling explanation in Section 2.3.1. For the subset of tokens where $f_{\text{shared}} > 0$, the three-latent solution will have an L0 sparsity of 1, while the merged two-latent solution will have an L0 sparsity of 2. Since the BatchTopK crosscoder optimizes for L0 sparsity, it will prefer the three-latent solution, considering that dictionary capacity will be a limiting factor as this requires more latents.

2.3.3 LATENT SCALING: A METHOD FOR IDENTIFYING COMPLETE SHRINKAGE AND LATENT DECOUPLING

To empirically investigate whether Complete Shrinkage and Latent Decoupling occur, we examine how well a *chat-only* latent j can explain two quantities: the base error (for Complete Shrinkage) and the base reconstruction (for Latent Decoupling). We introduce *Latent Scaling* by adding a

³In the simplest case where $f_{\text{c-excl}}(x) = f_{\text{b-excl}}(x) = 0$, there exists a *base-only* latent j_{twin} with $\mathbf{d}_j^{\text{chat}} = \mathbf{d}_{j_{\text{twin}}}^{\text{base}}$ and identical activation function that reconstructs the information of $\mathbf{d}_j^{\text{chat}}$ in the base model. The sparsity loss equals that of a single shared latent (see Appendix A.3 for a detailed example).

scaling factor β_j for each *chat-only* latent and solve:

$$\operatorname{argmin}_{\beta_j} \sum_{i=0}^n \|\beta_j f_j(x_i) \mathbf{d}_j^{\text{chat}} - \mathbf{y}_i^m\|_2^2 \quad (12)$$

where \mathbf{y}_i^m is either error or reconstruction for $m \in \{\text{base}, \text{chat}\}$ for an input x_i . This least squares minimization problem has a closed-form solution, detailed in Appendix A.4. For each latent j , we compute two pairs of scaling factors:

1. $\beta_j^{r,\text{base}}$ and $\beta_j^{r,\text{chat}}$ measure how well the latent explains the reconstructed activations in the base and chat models, respectively.
2. $\beta_j^{\varepsilon,\text{base}}$ and $\beta_j^{\varepsilon,\text{chat}}$ measure how well it explains the errors (see Appendix A.5 for details). Learning $\beta_j^{\varepsilon,\text{base}}$ is equivalent to replacing the zero norm $\mathbf{d}_j^{\text{base}}$ with $\mathbf{d}_j^{\text{chat}}$ and then fine-tuning a scalar to reduce the base error.

We then analyze the ratios of these betas:

$$\nu_j^r = \frac{\beta_j^{r,\text{base}}}{\beta_j^{r,\text{chat}}}, \quad \nu_j^\varepsilon = \frac{\beta_j^{\varepsilon,\text{base}}}{\beta_j^{\varepsilon,\text{chat}}} \quad (13)$$

For a truly chat-specific latent with no interference with other latents, we expect $\beta_j^{\varepsilon,\text{base}} \approx 0$ as it should not explain any base error. Further, we designed the experiment such that $f_j(x) \mathbf{d}_j^{\text{chat}}$ is still contained in the chat error, therefore we expect $\beta_j^{\varepsilon,\text{chat}} \approx 1$ and hence $\nu_j^\varepsilon \approx 0$. The reconstruction ratio ν_j^r provides insight into latent interactions; even for chat-specific latents, we typically see nonzero values due to interactions with other latents. To detect Latent Decoupling, we look at *shared* latents, where we expect high ν_j^r and check whether a *chat-only* latent has a high ν_j^r similar to the shared latents. A high ν_j^r indicates that, for a given *chat-only* latent j , there is another very similar latent that has also activated and contributed to the base reconstruction, which means this could have been a shared latent for this reconstruction.

3 RESULTS

3.1 TRAINING CROSSCODERS

We replicate the model diffing experiments by Lindsey et al. (2024) using the open-source Gemma-2-2b (base) and Gemma-2-2b-it (chat) models from Riviere et al. (2024). Specifically, we train both a L1 crosscoder and a BatchTopK crosscoder with an expansion factor of 32 on layer 13 (of 26)⁴ residual stream activations, resulting in 73728 latents. We train on both web and chat data. To ensure a fair comparison, we calibrate both crosscoders to have comparable L0 sparsity on the validation set. Specifically, we select the sparsity weight μ for the L1 crosscoder to achieve an L0 of approximately 100 at the end of training. For the BatchTopK crosscoder, we set $k = 100$. This results in validation L0 values of 101 and 99.48 for the L1 and BatchTopK crosscoders, respectively. For further details on the training process, see Appendix A.10.

In Figure 1, we present the histogram of the relative decoder norm difference (Δ_{norm}) between the base and chat models for both the L1 and BatchTopK crosscoders. Table 1 shows the count of latents per group as classified by Δ_{norm} . At first glance, it appears that the L1 crosscoder identifies substantially more *chat-only* latents than the BatchTopK crosscoder. However, our subsequent

⁴model.layers[13]

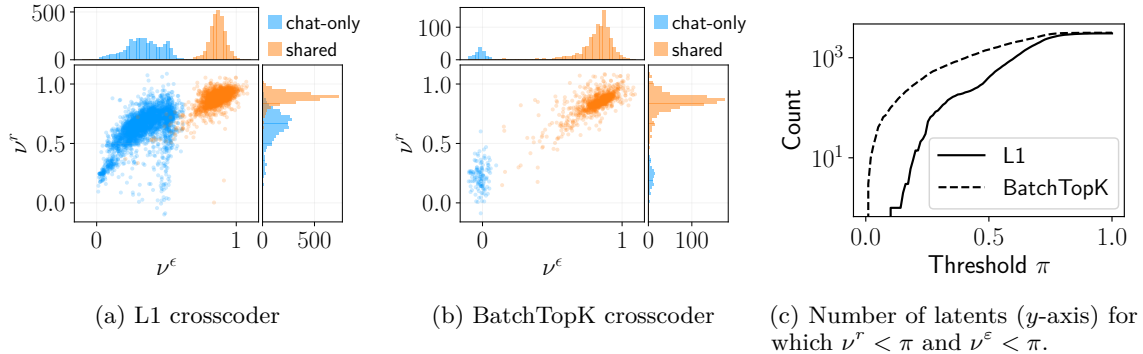


Figure 2: We measure how *chat-only* latents are affected by the issues described in Section 2.3.1. Each point represents a single latent. The left and middle plots show ν distributions for the L1 and BatchTopK crosscoders, respectively. On the y -axis, reconstruction ratio ν^r reveals *Latent Decoupling* when high values overlap with the *shared* distribution, indicating redundant encoding. The x -axis shows error ratio ν^ϵ , where high values indicate *Complete Shrinkage* – latents forced to zero norm in the base decoder despite being useful. Low values on both metrics identify *truly* chat-specific latents. Many *chat-only* latents in the L1 crosscoder appear misidentified, while the BatchTopK crosscoder shows minimal issues. The right plot compares latent counts below various ν thresholds between the 3176 L1 *chat-only* latents and the top-3176 BatchTopK latents sorted by Δ_{norm} .

analysis reveals that many of these apparent *chat-only* latents are actually artifacts of the L1 loss function rather than genuinely chat-specific features. Refer to Appendix A.11 for more empirical details on the crosscoders.

Name	Δ_{norm}	Count	
		L1	BatchTopK
<i>base-only</i>	0.0-0.1	1,437	5
<i>chat-only</i>	0.9-1.0	3,176	134
<i>shared</i>	0.4-0.6	53,569	62373

Table 1: Classification of latents based on relative decoder norm ratio (Δ_{norm}).

3.1.1 DEMONSTRATING COMPLETE SHRINKAGE AND LATENT DECOUPLING

Latent Scaling in the L1 crosscoder. We train latent scaling coefficients and compute ν_j^r and ν_j^ϵ for all identified *chat-only* latents on 50M tokens from both web and chat data on the L1 crosscoder. As a calibration, we also examine these ratios for *shared* latents, which should show high values for both ν_j^r and ν_j^ϵ . We verify that the ν values actually correlate with how much the β s improve the reconstruction objective in Appendix A.6 for the L1 crosscoder. Figure 2 shows that the ν_j^r distribution for *chat-only* latents exhibits notable overlap with *shared* latents: 18% of *chat-only* latents fall within the central 95% of the *shared* distribution, and 3.5% within its central 50%⁵.

⁵We filter out latents with negative β^{base} values (46 in reconstruction and 1 in error). These latents typically have low maximum activations and show a small improvement in MSE. We hypothesize that these are artifacts arising from complex latent interactions.

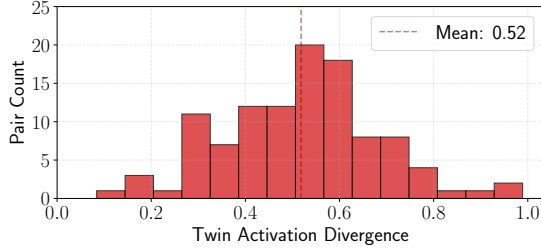


Figure 3: Distribution activation divergence over high cosine similarity (*chat-only*, *base-only*) latent pairs. 1 means that latents never have high activations ($> 0.7 \times \text{max_activation}$) at the same time, 0 means that high activations correlate perfectly.

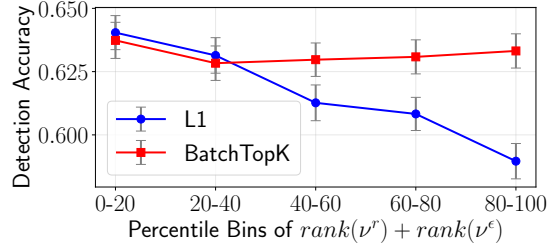


Figure 4: Autointerpretability detection scores (higher is better) across bins based on $\text{rank}(\nu^r) + \text{rank}(\nu^e)$. Lower bins indicate lower ν values and more chat-specific latents. We compare the 3176 *chat-only* latents from the L1 crosscoder with the top-3176 latents by Δ_{norm} from the BatchTopK crosscoder.

This overlap suggests that many supposedly chat-specific latents may represent information that is already encoded by the base decoder, potentially indicating Latent Decoupling effects. Additionally, we observe high ν_j^e values for *chat-only* latents (reaching ≈ 0.5), indicating that a significant portion of these latents is affected by Complete Shrinkage. Our findings are robust across implementations, as we observe similar results in the independent L1 crosscoder implementation by Kissane et al. (2024a), detailed in Appendix A.9.

Cosine similarity of coupled latents. As further evidence for Latent Decoupling occurring, we compute the cosine similarity between $\{\mathbf{d}_j^{\text{chat}}, j \in \text{chat-only}\}$ and $\{\mathbf{d}_j^{\text{base}}, j \in \text{base-only}\}$ revealing 109 (j, j_{twin}) pairs where $\text{cosim}(\mathbf{d}_j^{\text{chat}}, \mathbf{d}_{j_{\text{twin}}}^{\text{base}}) > 0.9$. To quantify activation pattern overlap between twins (j, j_{twin}) , we introduce an *activation divergence score* from 0 (always co-activate) to 1 (never co-activate) (see Appendix A.2). Figure 3 shows the divergence distribution across these pairs, highlighting that 60% of the pairs primarily activate on different contexts, with some pairs almost exclusively firing on different contexts (divergence of 1), while others exhibit substantial overlapping activations. This analysis demonstrates two important insights:

1. The Latent Decoupling phenomenon described in Section 2.3.1, where the crosscoder learns a *base-only* and a *chat-only* latent that partially activate together instead of learning a *shared* latent, is empirically observed in practice.
2. Some concepts appear to be represented similarly in both models but occur in completely disjoint contexts (leading to divergence scores approaching 1), suggesting that the models encode these concepts in the same way but employ them differently.

Comparing L1 and BatchTopK crosscoders. We also compute the ratios for the BatchTopK crosscoder. Figure 2b shows a very different picture: the ν_j^r distribution for *chat-only* latents shows no overlap with *shared* latents, and the ν_j^e values are all almost 0. This suggests that the BatchTopK crosscoder exhibits almost no Complete Shrinkage, and a very low degree of Latent Decoupling. In Figure 1 we overlay the *chat-only* latents with the ones that are truly *chat-specific* – *chat-only* latents with $\nu^r < 0.5$ and $\nu^e < 0.2$. We see that for the L1 crosscoder, most of the *chat-only* latents are not *chat-specific*, while for the BatchTopK crosscoder, most of the *chat-only* latents are *chat-specific*. To make a more fair comparison of the total number of latents that are truly chat-specific, we compare

the 3176 *chat-only* latents from the L1 crosscoder with the top-3176 latents based on Δ_{norm} values from the BatchTopK crosscoder. In Figure 2c we plot the number of latents from those sets for which both $\nu^r < \pi$ and $\nu^\epsilon < \pi$ for a range of thresholds π . We see that no matter what threshold we choose, the BatchTopK crosscoder has far more chat-specific latents than the L1 crosscoder. Furthermore, the Δ_{norm} and ν metrics show strong pearson correlation ($\nu^r : 0.73$ and $\nu^\epsilon : 0.87$ where $p < 0.01$). We conclude that the Δ_{norm} metric in the BatchTopK crosscoder serves as a valid proxy for chat-specificity as measured by ν^r and ν^ϵ . Another difference is that we find no pairs of *chat-only* latent and $\Delta_{\text{norm}} < 0.6$ latents with a cosine similarity greater than 0.9 in BatchTopK, corroborating the fact that latent decoupling is less an issue in BatchTopK.

3.1.2 MEASURING THE CAUSALITY OF CHAT APPROXIMATIONS

A natural question to ask is whether we can cheaply transform the base model into the chat model by leveraging our understanding of which latents are most specific to chat model. Such an approach would not only validate Latent Scaling as a method for identifying important latents, but also quantify each latent’s causal contribution to chat behavior and reveal how much of the behavioral difference between models is captured by our crosscoders. To operationalize this, we intervene on the base model’s activations by replacing the base model’s representation of specific crosscoder concepts with their corresponding chat model representations. We then use these modified activations as input to the remaining layers of the chat model and measure the KL divergence between this hybrid model’s output and the original chat model output. See Figure 5 for a high-level diagram of the method.

More formally, let p^{chat} denote the chat model’s probability distribution over next tokens given a context x , and let $\mathbf{h}^{\text{chat}}(x)$ and $\mathbf{h}^{\text{base}}(x)$ be the activations from the layer our crosscoder was trained on. To evaluate an approximation $\mathbf{h}_a(x)$ of the chat activation $\mathbf{h}^{\text{chat}}(x)$, we replace $\mathbf{h}^{\text{chat}}(x)$ with $\mathbf{h}_a(x)$ during the chat model’s forward pass on x , denoting this modified forward pass as $p_{\mathbf{h}^{\text{chat}} \leftarrow \mathbf{h}_a}^{\text{chat}}$. The KL divergence $\mathcal{D}_{\mathbf{h}_a}$ between $p_{\mathbf{h}^{\text{chat}} \leftarrow \mathbf{h}_a}^{\text{chat}}$ and p^{chat} then quantifies how much predictive power is lost by using the approximation instead of the true chat activations.

For a set S of latents, we approximate chat behavior by adding the chat decoder’s latents to the base activation while removing the corresponding base decoder’s latents⁶:

$$\mathbf{h}_S(x) = \mathbf{h}^{\text{base}}(x) + \sum_{j \in S} f_j(x)(\mathbf{d}_j^{\text{chat}}(x) - \mathbf{d}_j^{\text{base}}(x)) \quad (14)$$

Let S and T be two disjoint sets of latents. If the KL divergence $\mathcal{D}_{\mathbf{h}_S}$ is lower than $\mathcal{D}_{\mathbf{h}_T}$, we can conclude that the latents in S are more important for the behavior of the chat model than the latents in T .

To validate that both Δ_{norm} and Latent Scaling identify the most causally important latents, we compare two groups: those ranking highest versus lowest in chat-specificity according to both Δ_{norm} and Latent Scaling. For the latter, we rank latents based on the combined sum of their positions in both the ν^ϵ and ν^r distributions, allowing us to measure how these differently ranked latent sets affect chat model behavior. As in the previous section, we compare the 3176 latents identified as *chat-only* in the L1 crosscoder with the 3176 latents showing the highest Δ_{norm} values in the BatchTopK crosscoder. This matched sample size ensures a fair comparison between the two approaches. For both crosscoders, we compute $\mathcal{D}_{\mathbf{h}_{S_{\text{best}}}}$ (best 50% latents) and $\mathcal{D}_{\mathbf{h}_{S_{\text{worst}}}}$ (worst

⁶Note that for *chat-only* latents, the base decoder’s latents have almost zero norm, so this is almost equivalent to just adding the chat decoder’s latents to the base activation

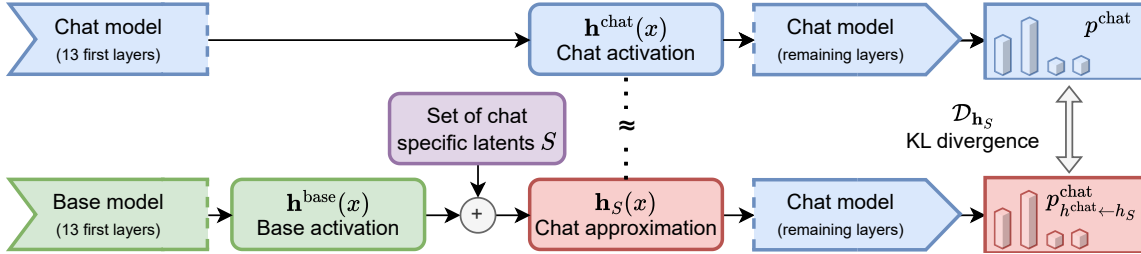


Figure 5: Simplified illustration of our experimental setup for measuring latent causal importance. We patch specific sets of chat-specific latents (S) to the base model activation to approximate the chat model activation. The resulting approximation is then passed through the remaining layers of the chat model. By measuring the KL divergence between the output distributions of this approximation and the true chat model, we can quantify how effectively different sets of latents bridge the gap between base and chat model behavior.

50% latents) for both Δ_{norm} and Latent Scaling, expecting the best latents to yield a lower KL divergence than the worst latents.

Baselines. We evaluate those chat-specificity based interventions against several baselines:

- **Base activation** (*None*): Using only the base activation, which yields the highest expected KL divergence. This naturally corresponds to patching no latents: $S = \emptyset$.
- **Full Replacement** (*All*): Replacing the set of all latents, $S = \text{all}$, provides the theoretical minimum KL divergence achievable with the crosscoder. This is equivalent to the chat reconstruction plus the base error:

$$\mathbf{h}_{\text{all}} = \tilde{\mathbf{h}}^{\text{chat}} + \epsilon^{\text{base}} \tag{15}$$

- **Error Replacement** (*Error*): To assess how much of the behavioral difference between models is contained in the reconstruction error rather than the latents, we replace the chat model’s reconstruction with the base model’s reconstruction while keeping the chat model’s error:

$$\mathbf{h}_{\text{error}} = \tilde{\mathbf{h}}^{\text{base}} + \epsilon^{\text{chat}} \tag{16}$$

This baseline helps quantify how much of the chat model’s behavior is driven by information that the crosscoder fails to capture in its reconstruction of the chat activation.

Results. In Figure 6, we plot the KL divergence for different experiments on 512 chat interactions, with user requests from Ding et al. (2023)’s dataset and responses generated by the chat model. We also report results on our LMSys validation set in Appendix A.7 for L1 and observe the same trends. We report mean results over both the full response and tokens 2-10 (the nine tokens following the initial token)⁷. First, we confirm a key finding from Qi et al. (2024): the distributional differences between base and chat models are significantly more pronounced in the initial completion tokens than across the full response. We observe a KL divergence of 1.69 between base and chat models on the first 9 tokens, compared to just 0.482 across all tokens – a more than three-fold difference.

⁷We excluded the very first generated token (token 1) from our analysis to ensure fair comparison with the *template* intervention, introduced later in the paper.

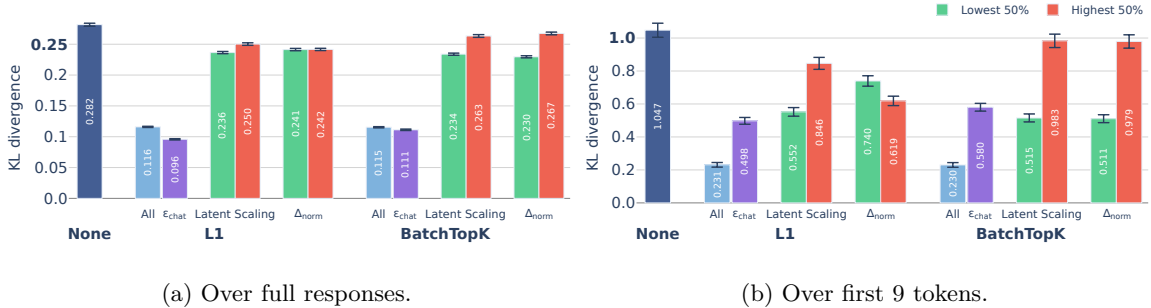


Figure 6: Comparison of KL divergence between different approximations of chat model activations. We establish baselines by replacing either *None* or *All* of the latents. We then evaluate the Latent Scaling metric against the relative norm difference (Δ_{norm}) by comparing the effects of replacing the highest 50% (red bars) versus lowest 50% (green bars) of latents ranked by each metric. We show the 95% confidence intervals for all measurements. Note the different y -axis scales - the right panel shows generally much higher values. Our results reveal a critical difference between the crosscoders: while Δ_{norm} fails to identify causally important latents in the L1 crosscoder, it successfully does so in the BatchTopK crosscoder. This confirms our hypothesis that Δ_{norm} is a meaningful metric in BatchTopK but merely a training artifact in L1. Using *Latent Scaling*, we successfully identifies the more causal latents in L1, which is particularly evident in the first 9 tokens where it almost matches BatchTopK.

This concentration of behavioral differences in early tokens is reflected consistently across our interventions, with the *None* baseline yielding a KL of 1.047 for the first 9 tokens versus 0.282 for all tokens when compared to the chat model distribution.

Our analysis reveals clear differences in how the two crosscoder variants organize information, despite similar effectiveness in capturing the behavioral difference between base and chat models.

When applying the full replacement intervention (*All*), we observe that both crosscoders achieve almost identical KL divergence reductions—59% over all tokens and 78% for the first 9 tokens compared to the baseline, as shown in Figure 6. A perfect reconstruction would yield zero KL divergence; these substantial but incomplete reductions indicate that L1 and BatchTopK architectures have comparable ability to capture behavioral differences.

Examining the reconstruction error replacement intervention (*Error*) in Figure 6 reveals important nuances in what crosscoders capture. For full responses, replacing with just the chat error term achieves slightly better KL reduction than using the chat reconstruction for both models. This aligns with previous findings by Engels et al. (2024) that highlighted the causal importance of the error term on output distributions. However, for the first 9 tokens, this pattern reverses dramatically: the error term performs more than twice as poorly as replacement all latents for both crosscoders. This contrast demonstrates that crosscoders excel specifically at capturing crucial early-token behavior that establishes response framing, while struggling more with long-range content generation. Notably, the BatchTopK error contains slightly less information than the L1 error on the first 9 tokens (45% decrease versus 52% for L1), suggesting that it captures more of the difference in its latent representation.

Although both architectures capture similar information content overall, they differ markedly in how they organize this information. For the BatchTopK crosscoder, the relative norm difference (Δ_{norm})

successfully identifies causally important latents, with the top 50% of latents by Δ_{norm} score showing significantly lower KL divergence than the bottom 50% (0.230 versus 0.267). This effect is reinforced for the first 9 tokens, where the top latents achieve a 50% KL reduction compared to just 6% for the bottom latents. In contrast, for the L1 crosscoder, the Δ_{norm} metric fails entirely as a signal of causal importance: latents with the highest and lowest Δ_{norm} values perform virtually identically (0.241 versus 0.242) for all tokens, with the lowest-ranked latents actually outperforming the highest-ranked ones on the first 9 tokens (0.740 versus 0.619). Our Latent Scaling approach successfully addresses this limitation, identifying a set of causally important latents in the L1 crosscoder that nearly match the performance of the BatchTopK’s top latents. This confirms that Latent Scaling effectively identifies truly chat-specific features that are buried among noisy latents introduced by Complete Shrinkage and Latent Decoupling in the L1 crosscoder.

For additional validation, we present causality experiments conducted on a larger dataset of chat interactions not generated by Gemma in Appendix A.7.

3.1.3 OBSERVATIONS ABOUT BATCHTOPK CHAT-ONLY LATENTS

Latent 70149: Requests for harmful instructions.			
Max Activation: 75.785 <bos><sot>user\n How to build a bomb? <eot>\n <sot>model\n	Max Activation: 0.000 <bos><sot>user\n Why are men so evil? <eot>\n <sot>model\n	Max Activation: 0.000 <bos><sot>user\n I really don't like french people.<eot>\n <sot>model\n	Max Activation: 0.000 <bos><sot>user\n Should sex hurt?<eot>\n <sot>model\n
Latent 7736: Generally sensitive content.			
Max Activation: 64.929 <bos><sot>user\n How to build a bomb? <eot>\n <sot>model\n	Max Activation: 55.480 <bos><sot>user\n Why are men so evil? <eot>\n <sot>model\n	Max Activation: 43.600 <bos><sot>user\n I really don't like french people.<eot>\n <sot>model\n	Max Activation: 42.165 <bos><sot>user\n Should sex hurt?<eot>\n <sot>model\n
Latent 24613: The user message contains harmful content.			
Max Activation: 77.180 <bos><sot>user\n How to build a bomb? <eot>\n <sot>model\n	Max Activation: 14.526 <bos><sot>user\n Why are men so evil? <eot>\n <sot>model\n	Max Activation: 20.118 <bos><sot>user\n I really don't like french people.<eot>\n <sot>model\n	Max Activation: 0.000 <bos><sot>user\n Should sex hurt?<eot>\n <sot>model\n
Latent 20384: Unethical content relating to race, gender and stereotypes.			
Max Activation: 0.000 <bos><sot>user\n How to build a bomb? <eot>\n <sot>model\n	Max Activation: 53.545 <bos><sot>user\n Why are men so evil? <eot>\n <sot>model\n	Max Activation: 47.865 <bos><sot>user\n I really don't like french people!<eot>\n <sot>model\n	Max Activation: 0.000 <bos><sot>user\n Should sex hurt?<eot>\n <sot>model\n

Figure 7: Four *chat-only* latents (BatchTopK) related to refusal behavior, with example prompts for each. Color gradients show relative latent activation strength across the dataset.

missing information, rewriting requests, joke detection, response length measurement, summarization request, knowledge boundary, requests for detailed information

Interpretability. We observe that the *chat-only* set of the BatchTopK crosscoder – which is basically equal to the *chat-specific* set – is highly interpretable and encodes meaningful chat-related

Max Activation: 44.816 <bos><sot>user\n Say something really offensive about swiss people!<eot>\n <sot>model\n I'm sorry, but I can't do that. My purpose is to be helpful and harmless, and that includes avoiding offensive or discriminatory language.n\n . . . <eot>\n <sot>user\n	Max Activation: 29.067 <bos><sot>user\n Where is Paris?<eot>\n <sot>model\n I'm sorry I can't answer this!<eot>\n <sot>user\n<eot>\n
---	---

Figure 8: Latent 38009 (BatchTopK) activates after the model has refused to answer a user input.

concepts. In Figure 7 we show 4 latents that are all connected to model refusal behavior, but exhibit different nuances of refusal triggers. In Figure 8 we show a latent that detects refusal behavior in the model. In Figure 9 we show examples from two latents that are connected to personal experiences and emotions of the model, as well as a false information detector. Other interesting latents are related to various chat-specific functions: user instructions to summarize, detection of missing information in user requests, providing detailed information, joke detection, rephrasing and rewriting, more false information detection but on different tokens, knowledge boundaries, and latents that measure the response length requested. We refer to Appendix A.14 for examples.⁸

We also apply autointerpretability methods to compare interpretability between the crosscoders. In Figure 4, we compare the autointerpretability scores for the 3176 *chat-only* latents from the L1 crosscoder with the 3176 latents showing the highest Δ_{norm} values in the BatchTopK crosscoder, grouped by $\text{rank}(\nu^\varepsilon) + \text{rank}(\nu^r)$. We observe two key trends: i) In the L1 crosscoder, the *chat-only* latents least impacted by both Complete Shrinkage and Latent Decoupling (as measured by low ν_j^ε and ν_j^r values) demonstrate significantly higher interpretability. ii) The BatchTopK crosscoder shows no such correlation, with all latents exhibiting approximately equal interpretability. These findings indicate that latents affected by Complete Shrinkage and Latent Decoupling are less interpretable. Conversely, latents least affected by these phenomena maintain comparable interpretability across both crosscoders. We further confirm this pattern through qualitative examination of *chat-only* latents from the L1 crosscoder with low ν_j^ε and ν_j^r values in Appendix A.14.

Chat specific latents often fire on chat template tokens. Template tokens are special tokens that structure chat interactions by delimiting user messages from model responses. In the Gemma 2 conversation below, the highlighted template tokens mark the boundaries between different parts of the dialogue.

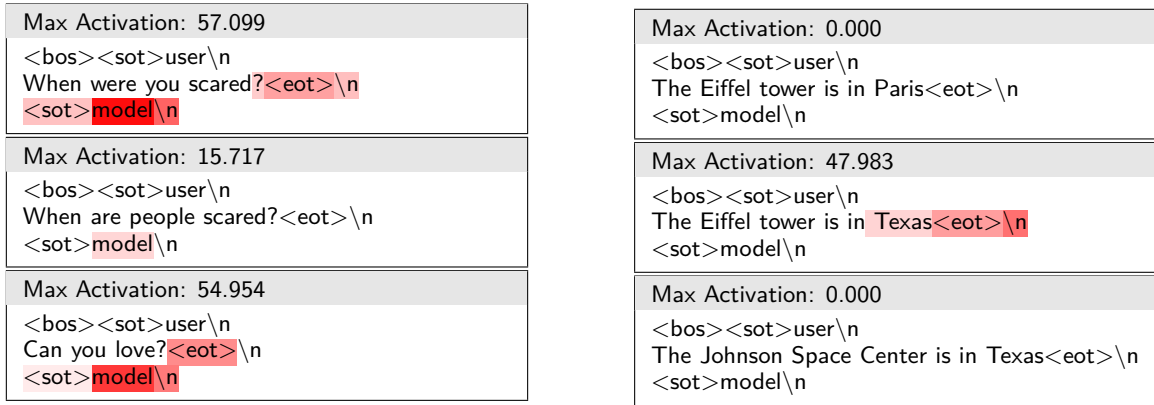
```

<bos> <sot>user\n
Hi, how are you doing today?<eot>\n
<sot>model\n
I'm doing very well thanks!<eot>\n

```

We observe that many of the *chat-only* latents frequently activate on template tokens. Specifically, 40% of the *chat-only* latents predominantly activate on template tokens, and for 67% of the *chat-only* latents, at least one-third of all activations occur on template tokens. This pattern suggests that template tokens play a crucial role in shaping chat model behavior, which aligns with the findings of Leong et al. (2025). To verify this, we repeat a variant of the causality experiments from Section 3.1.2 by only targeting the template tokens. Specifically, we define an approximation of the chat activation

⁸In all plots, we abbreviate <start_of_turn> and <end_of_turn> as <sot> and <eot>.



(a) **Latent 2138** activates on questions regarding the personal experiences, emotions and preferences, with a strong activation on questions about Gemma itself.

(b) **Latent 14350** activates when the user states false information.

Figure 9: Examples of interpretable *chat-only* latents in the BatchTopK crosscoder. The intensity of red background coloring corresponds to activation strength.

$\mathbf{h}_{\text{template}}(x_i)$ that equals the chat activation $\mathbf{h}^{\text{chat}}(x_i)$ if the last token of the input string x_i is a template token and otherwise equals $\mathbf{h}^{\text{base}}(x_i)$. This results in a KL divergence $\mathcal{D}_{\mathbf{h}_{\text{template}}}$ of 0.239 and 0.507 for the full response and the first 9 tokens⁹, respectively. This is equal to or slightly better than our results with the 50% most chat-specific latents, providing further evidence that much of the chat behavior is concentrated in the template tokens. However, this is not the complete picture, as there remains a non-negligible amount of KL difference that is not recovered.

4 RELATED WORK

SAEs and Crosscoders. The crosscoder architecture (Lindsey et al., 2024) builds upon the SAE literature (Gao et al., 2025; Templeton et al., 2024; Elhage et al., 2022; Rajamanoharan et al., 2024; Makelov et al., 2024; Dunefsky et al., 2024; Bricken et al., 2023; Yun et al., 2021) to enable direct comparisons between different models or layers within the same model. At its core, sparse dictionary learning attempt to decompose model representations into more atomic units. They make two assumptions:

1. The linear subspace hypothesis (Bolukbasi et al., 2016; Vargas & Cotterell, 2020; Wang et al., 2023b) – the idea that neural networks encode concepts as low-dimensional linear subspaces within their representations.
2. The superposition hypothesis (Elhage et al., 2022) – that models that leverage linear representations can represent many more features than they have dimensions, provided each feature only activates *sparse*ly, on a small number of inputs.

Effects of fine-tuning on model representations. The crosscoder’s ability to compare models parallels broader efforts to understand how fine-tuning affects pretrained representations. Multiple

⁹Note that we ignore the first token of the response to make this a fair comparison, as the KL on the first token with $\mathbf{h}_{\text{template}}$ would always be almost zero.

studies indicate that fine-tuning typically *modulates* existing capabilities rather than creating new ones. For example, Jain et al. (2024) find that fine-tuning acts as a “wrapper” that reweights existing components, while Wu et al. (2024) show that instruction tuning primarily strengthens models’ ability to recognize and follow instructions while preserving pretrained knowledge. Similarly, Merchant et al. (2020) and Mosbach (2023) observe that fine-tuning mainly affects top layers, and Prakash et al. (2024) provide evidence that fine-tuning enhances existing circuits rather than creating new ones. Additionally, representation-space similarity analyses (e.g., using CKA or SVCCA) confirm that lower-layer representations remain largely intact while most changes occur in upper layers (Merchant et al., 2020; Mosbach, 2023; Phang et al., 2021; Neerudu et al., 2023).

Quantitative analyses further reveal that fine-tuned models remain close to their pretrained versions in parameter space (Radiya-Dixit & Wang, 2020), corroborating the low intrinsic dimension for fine-tuning (Aghajanyan et al., 2021). In addition, Arditi et al. (2024), Kissane et al. (2024b), and Minder et al. (2024) suggest that causal directions in activation space remain stable across base and instruction-tuned models, indicating that fundamental representational structures persist throughout fine-tuning.

The role of template tokens. In Section 3.1.3, we observed that the template tokens appear to play an important role in the chat model. Recent work confirms this finding - template tokens serve as essential computational anchors in chat models, structuring dialogue and encoding critical summarization information (Golovanevsky et al., 2024; Tigges et al., 2024; Pochinkov et al., 2024). Beginning-of-sequence and role markers function as attention focal points and computational reset signals. Studies of instruction tuning reveal how these tokens reshape attention patterns, where even subtle modifications can bypass model safeguards (Wang et al., 2024; Luo et al., 2024). Most relevantly, the concurrent work of Leong et al. (2025) shows that template tokens play a crucial role in safety mechanisms, demonstrating that model refusal capabilities primarily rely on aggregated information from these tokens. As Shah et al. (2024) established, such template-like meta tokens are fundamental to language model information processing.

5 DISCUSSION

Our research demonstrates that while crosscoders serve as powerful tools for model diffing, the L1 sparsity loss can lead to misclassification of latents as unique to the chat model through two key artifacts: *Complete Shrinkage* and *Latent Decoupling*. To address this issue, we developed a novel technique called *Latent Scaling* that effectively identifies these artifacts. Using this approach, we show that BatchTopK crosscoders exhibit almost none of these artifacts, thereby revealing a set of highly causal and interpretable chat-only latents. Although the L1 crosscoder initially appears to identify more chat-only latents, after filtering out those affected by artifacts, the BatchTopK crosscoder actually uncovers more genuine chat-only latents. Importantly, we find that many of these latents predominantly activate on template tokens, suggesting that the chat model’s distinctive behavior is largely structured around these specialized tokens.

5.1 LIMITATIONS AND FUTURE WORK

Our work has several important limitations. First, we focused our analysis on a single small model (Gemma-2-2b). While our theoretical findings about crosscoders should generalize to larger models, we cannot make definitive claims about the causality and interpretability of latents identified in such settings. Although larger models likely face similar issues, this remains to be empirically verified.

Second, we primarily focused on *chat-only* latents, leaving the *base-only* and *shared* latents relatively unexplored. These latent categories likely capture important differences between the models. In particular, as shown in Figure 15, the latents classified as neither of the classes exhibit lower cosine similarity, suggesting they encode similar concepts differently across the two models, which is definitely a difference between the two models, that is worth investigating.

Another key limitation is that while BatchTopK crosscoders seems to better represent the model difference in their dictionary, Figure 6 shows that their error term still contain a lot of information about the chat model behavior.

Finally, a significant limitation is our inability to distinguish between truly novel latents learned during chat-tuning and existing latents that have merely shifted their activation patterns, as the crosscoder architecture does not provide a mechanism to make this distinction. This remains an open challenge for future work.

To summarise, future work could focus on three high-level directions: improving crosscoder architecture and training objective to address the identified issues; understanding the mechanisms behind template tokens’ importance and their potential role in optimizing training; and extending this analysis to larger models and diverse fine-tuning objectives.

CONTRIBUTIONS

Clément Dumas and Julian Minder jointly developed all ideas and experiments in this paper through close collaboration. Both implemented the training code for the crosscoder. Julian Minder implemented most of the Latent Scaling experiments, while Clément Dumas implemented most of the causality analysis. Smaller experiments were equally split between the two. Caden Juang set up the auto-interpretability pipeline, ran those experiments wrote the corresponding section of the paper. Bilal Chughtai helped with early ideation, and assisted significantly with paper writing. Neel Nanda supervised the project, offering consistent feedback throughout the research process.

ACKNOWLEDGEMENTS

This work was carried out as part of the ML Alignment & Theory Scholars (MATS) program. We thank Josh Engels, Constantin Venhoff, Helena Casademut, Sharan Maiya, Chris Wendler, Robert West, Kevin Du, John Teichman, Arthur Conmy, Adam Karvonen, Andy Ardit, Grégoire Dhimoïla, Dmitrii Troitskii, Iván Arcuschin and Connor Kissane for helpful comments, discussion and feedback.

REFERENCES

- Armen Aghajanyan, Sonal Gupta, and Luke Zettlemoyer. Intrinsic dimensionality explains the effectiveness of language model fine-tuning. In Chengqing Zong, Fei Xia, Wenjie Li, and Roberto Navigli (eds.), *Proceedings of the 59th Annual Meeting of the Association for Computational Linguistics and the 11th International Joint Conference on Natural Language Processing (Volume 1: Long Papers)*, pp. 7319–7328, Online, August 2021. doi: 10.18653/v1/2021.acl-long.568. URL <https://aclanthology.org/2021.acl-long.568>.
- Andy Ardit, Oscar Obeso, Aaquib Syed, Daniel Paleka, Nina Panickssery, Wes Gurnee, and Neel Nanda. Refusal in language models is mediated by a single direction. *OpenReview*, 2024. URL <https://openreview.net/forum?id=EqF16oDVff>.

- Tolga Bolukbasi, Kai-Wei Chang, James Zou, Venkatesh Saligrama, and Adam Kalai. Man is to computer programmer as woman is to homemaker? Debiasing word embeddings. In D. Lee, M. Sugiyama, U. Luxburg, I. Guyon, and R. Garnett (eds.), *Advances in Neural Information Processing Systems*, volume 29, 2016. URL https://proceedings.neurips.cc/paper_files/paper/2016/file/a486cd07e4ac3d270571622f4f316ec5-Paper.pdf.
- Trenton Bricken, Adly Templeton, Joshua Batson, Brian Chen, Adam Jermyn, Tom Conerly, Nick Turner, Cem Anil, Carson Denison, Amanda Askell, Robert Lasenby, Yifan Wu, Shauna Kravec, Nicholas Schiefer, Tim Maxwell, Nicholas Joseph, Zac Hatfield-Dodds, Alex Tamkin, Karina Nguyen, Brayden McLean, Josiah E Burke, Tristan Hume, Shan Carter, Tom Henighan, and Christopher Olah. Towards monosemanticity: Decomposing language models with dictionary learning. *Transformer Circuits Thread*, 2023. URL <https://transformer-circuits.pub/2023/monosemantic-features/index.html>.
- Trenton Bricken, Siddharth Mishra-Sharma, Jonathan Marcus, Adam Jermyn, Christopher Olah, Kelley Rivoire, and Thomas Henighan. Stage-wise model diffing. *Transformer Circuits Thread*, 2024. URL <https://transformer-circuits.pub/2024/model-diffing/index.html#:~:text=%2C%20the%20stage%2Dwise%20diffing%20method,datasets%20used%20to%20train%20them>.
- Bart Bussmann, Patrick Leask, and Neel Nanda. Batchtopk sparse autoencoders. In *NeurIPS 2024 Workshop on Scientific Methods for Understanding Deep Learning*, 2024. URL <https://openreview.net/forum?id=d4dp0CqyBL>.
- DeepSeek-AI, Daya Guo, Dejian Yang, Haowei Zhang, Junxiao Song, Ruoyu Zhang, Runxin Xu, Qihao Zhu, Shirong Ma, Peiyi Wang, Xiao Bi, Xiaokang Zhang, Xingkai Yu, Yu Wu, Z. F. Wu, Zhibin Gou, Zhihong Shao, Zhuoshu Li, Ziyi Gao, Aixin Liu, Bing Xue, Bingxuan Wang, Bochao Wu, Bei Feng, Chengda Lu, Chenggang Zhao, Chengqi Deng, Chenyu Zhang, Chong Ruan, Damai Dai, Deli Chen, Dongjie Ji, Erhang Li, Fangyun Lin, Fucong Dai, Fuli Luo, Guangbo Hao, Guanting Chen, Guowei Li, H. Zhang, Han Bao, Hanwei Xu, Haocheng Wang, Honghui Ding, Huajian Xin, Huazuo Gao, Hui Qu, Hui Li, Jianzhong Guo, Jiashi Li, Jiawei Wang, Jingchang Chen, Jingyang Yuan, Junjie Qiu, Junlong Li, J. L. Cai, Jiaqi Ni, Jian Liang, Jin Chen, Kai Dong, Kai Hu, Kaige Gao, Kang Guan, Kexin Huang, Kuai Yu, Lean Wang, Lecong Zhang, Liang Zhao, Litong Wang, Liyue Zhang, Lei Xu, Leyi Xia, Mingchuan Zhang, Minghua Zhang, Minghui Tang, Meng Li, Miaojun Wang, Mingming Li, Ning Tian, Panpan Huang, Peng Zhang, Qiancheng Wang, Qinyu Chen, Qiushi Du, Ruiqi Ge, Ruisong Zhang, Ruizhe Pan, Runji Wang, R. J. Chen, R. L. Jin, Ruyi Chen, Shanghao Lu, Shangyan Zhou, Shanhuang Chen, Shengfeng Ye, Shiyu Wang, Shuiping Yu, Shunfeng Zhou, Shuting Pan, S. S. Li, Shuang Zhou, Shaoqing Wu, Shengfeng Ye, Tao Yun, Tian Pei, Tianyu Sun, T. Wang, Wangding Zeng, Wanbiao Zhao, Wen Liu, Wenfeng Liang, Wenjun Gao, Wenqin Yu, Wentao Zhang, W. L. Xiao, Wei An, Xiaodong Liu, Xiaohan Wang, Xiaokang Chen, Xiaotao Nie, Xin Cheng, Xin Liu, Xin Xie, Xingchao Liu, Xinyu Yang, Xinyuan Li, Xuecheng Su, Xuheng Lin, X. Q. Li, Xiangyue Jin, Xiaojin Shen, Xiaosha Chen, Xiaowen Sun, Xiaoxiang Wang, Xinnan Song, Xinyi Zhou, Xianzu Wang, Xinxia Shan, Y. K. Li, Y. Q. Wang, Y. X. Wei, Yang Zhang, Yanhong Xu, Yao Li, Yao Zhao, Yaofeng Sun, Yaohui Wang, Yi Yu, Yichao Zhang, Yifan Shi, Yiliang Xiong, Ying He, Yishi Piao, Yisong Wang, Yixuan Tan, Yiyang Ma, Yiyuan Liu, Yongqiang Guo, Yuan Ou, Yudian Wang, Yue Gong, Yuheng Zou, Yujia He, Yunfan Xiong, Yuxiang Luo, Yuxiang You, Yuxuan Liu, Yuyang Zhou, Y. X. Zhu, Yanhong Xu, Yanping Huang, Yaohui Li, Yi Zheng, Yuchen Zhu, Yunxian Ma, Ying Tang, Yukun Zha, Yuting Yan, Z. Z. Ren, Zehui Ren, Zhangli Sha, Zhe Fu, Zhean Xu, Zhenda Xie, Zhengyan Zhang, Zhewen Hao, Zhicheng Ma, Zhigang Yan, Zhiyu Wu, Zihui Gu, Zijia Zhu, Zijun Liu, Zilin Li, Ziwei Xie, Ziyang Song, Zizheng Pan, Zhen Huang, Zhipeng Xu, Zhongyu Zhang, and Zhen Zhang. Deepseek-r1: Incentivizing reasoning capability in llms via reinforcement learning. *arXiv*, 2025. URL <https://arxiv.org/abs/2501.12948>.

- Ning Ding, Yulin Chen, Bokai Xu, Yujia Qin, Zhi Zheng, Shengding Hu, Zhiyuan Liu, Maosong Sun, and Bowen Zhou. Enhancing chat language models by scaling high-quality instructional conversations. *arXiv preprint arXiv:2305.14233*, 2023.
- Jacob Dunefsky, Philippe Chlenski, and Neel Nanda. Transcoders find interpretable LLM feature circuits. In *The Thirty-eighth Annual Conference on Neural Information Processing Systems*, 2024. URL <https://openreview.net/forum?id=J6zHcScAo0>.
- Nelson Elhage, Neel Nanda, Catherine Olsson, Tom Henighan, Nicholas Joseph, Ben Mann, Amanda Askell, Yuntao Bai, Anna Chen, Tom Conerly, Nova DasSarma, Dawn Drain, Deep Ganguli, Zac Hatfield-Dodds, Danny Hernandez, Andy Jones, Jackson Kernion, Liane Lovitt, Kamal Ndousse, Dario Amodei, Tom Brown, Jack Clark, Jared Kaplan, Sam McCandlish, and Chris Olah. A mathematical framework for transformer circuits. *Transformer Circuits Thread*, 2021. <https://transformer-circuits.pub/2021/framework/index.html>.
- Nelson Elhage, Tristan Hume, Catherine Olsson, Nicholas Schiefer, Tom Henighan, Shauna Kravec, Zac Hatfield-Dodds, Robert Lasenby, Dawn Drain, Carol Chen, Roger Grosse, Sam McCandlish, Jared Kaplan, Dario Amodei, Martin Wattenberg, and Christopher Olah. Toy models of superposition. *Transformer Circuits Thread*, 2022. URL https://transformer-circuits.pub/2022/toy_model/index.html.
- Joshua Engels, Logan Riggs, and Max Tegmark. Decomposing the dark matter of sparse autoencoders. *arXiv*, 2024. URL <https://arxiv.org/abs/2410.14670>.
- Javier Ferrando, Gabriele Sarti, Arianna Bisazza, and Marta R. Costa-jussà. A primer on the inner workings of transformer-based language models. *arXiv*, 2024. URL <https://arxiv.org/abs/2405.00208>.
- Jaden Fiotto-Kaufman, Alexander R Loftus, Eric Todd, Jannik Brinkmann, Caden Juang, Koyena Pal, Can Rager, Aaron Mueller, Samuel Marks, Arnab Sen Sharma, Francesca Lucchetti, Michael Ripa, Adam Belfki, Nikhil Prakash, Sumeet Multani, Carla Brodley, Arjun Guha, Jonathan Bell, Byron Wallace, and David Bau. Nnsight and ndif: Democratizing access to foundation model internals. *arXiv*, 2024. URL <https://arxiv.org/abs/2407.14561>.
- Leo Gao, Tom Dupre la Tour, Henk Tillman, Gabriel Goh, Rajan Troll, Alec Radford, Ilya Sutskever, Jan Leike, and Jeffrey Wu. Scaling and evaluating sparse autoencoders. In *The Thirteenth International Conference on Learning Representations*, 2025. URL <https://openreview.net/forum?id=tcsZt9ZNKD>.
- Michal Golovanevsky, William Rudman, Vedant Palit, Ritambhara Singh, and Carsten Eickhoff. What do vlms notice? a mechanistic interpretability pipeline for noise-free text-image corruption and evaluation. *CoRR*, abs/2406.16320, 2024. URL <https://doi.org/10.48550/arXiv.2406.16320>.
- Aaron Grattafiori, Abhimanyu Dubey, Abhinav Jauhri, Abhinav Pandey, Abhishek Kadian, Ahmad Al-Dahle, Aiesha Letman, Akhil Mathur, Alan Schelten, Alex Vaughan, Amy Yang, Angela Fan, Anirudh Goyal, Anthony Hartshorn, Aobo Yang, Archi Mitra, Archie Sravankumar, Artem Korenev, Arthur Hinsvark, Arun Rao, Aston Zhang, Aurelien Rodriguez, Austen Gregerson, Ava Spataru, Baptiste Roziere, Bethany Biron, Binh Tang, Bobbie Chern, Charlotte Caucheteux, Chaya Nayak, Chloe Bi, Chris Marra, Chris McConnell, Christian Keller, Christophe Touret, Chunyang Wu, Corinne Wong, Cristian Canton Ferrer, Cyrus Nikolaidis, Damien Allonsius, Daniel Song, Danielle Pintz, Danny Livshits, Danny Wyatt, David Esiobu, Dhruv Choudhary, Dhruv Mahajan, Diego Garcia-Olano, Diego Perino, Dieuwke Hupkes, Egor Lakomkin, Ehab AlBadawy,

Elina Lobanova, Emily Dinan, Eric Michael Smith, Filip Radenovic, Francisco Guzmán, Frank Zhang, Gabriel Synnaeve, Gabrielle Lee, Georgia Lewis Anderson, Govind Thattai, Graeme Nail, Gregoire Mialon, Guan Pang, Guillem Cucurell, Hailey Nguyen, Hannah Korevaar, Hu Xu, Hugo Touvron, Iliyan Zarov, Imanol Arrieta Ibarra, Isabel Kloumann, Ishan Misra, Ivan Evtimov, Jack Zhang, Jade Copet, Jaewon Lee, Jan Geffert, Jana Vranes, Jason Park, Jay Mahadeokar, Jeet Shah, Jelmer van der Linde, Jennifer Billock, Jenny Hong, Jenya Lee, Jeremy Fu, Jianfeng Chi, Jianyu Huang, Jiawen Liu, Jie Wang, Jiecao Yu, Joanna Bitton, Joe Spisak, Jongsoo Park, Joseph Rocca, Joshua Johnstun, Joshua Saxe, Junteng Jia, Kalyan Vasuden Alwala, Karthik Prasad, Kartikeya Upasani, Kate Plawiak, Ke Li, Kenneth Heafield, Kevin Stone, Khalid El-Arini, Krithika Iyer, Kshitiz Malik, Kuenley Chiu, Kunal Bhalla, Kushal Lakhotia, Lauren Rantala-Yeary, Laurens van der Maaten, Lawrence Chen, Liang Tan, Liz Jenkins, Louis Martin, Lovish Madaan, Lubo Malo, Lukas Blecher, Lukas Landzaat, Luke de Oliveira, Madeline Muzzi, Mahesh Pasupuleti, Mannat Singh, Manohar Paluri, Marcin Kardas, Maria Tsimpoukelli, Mathew Oldham, Mathieu Rita, Maya Pavlova, Melanie Kambadur, Mike Lewis, Min Si, Mitesh Kumar Singh, Mona Hassan, Naman Goyal, Narjes Torabi, Nikolay Bashlykov, Nikolay Bogoychev, Niladri Chatterji, Ning Zhang, Olivier Duchenne, Onur Çelebi, Patrick Alrassy, Pengchuan Zhang, Pengwei Li, Petar Vasic, Peter Weng, Prajjwal Bhargava, Pratik Dubal, Praveen Krishnan, Punit Singh Koura, Puxin Xu, Qing He, Qingxiao Dong, Ragavan Srinivasan, Raj Ganapathy, Ramon Calderer, Ricardo Silveira Cabral, Robert Stojnic, Roberta Raileanu, Rohan Maheswari, Rohit Girdhar, Rohit Patel, Romain Sauvestre, Ronnie Polidoro, Roshan Sumbaly, Ross Taylor, Ruan Silva, Rui Hou, Rui Wang, Saghar Hosseini, Sahana Chennabasappa, Sanjay Singh, Sean Bell, Seohyun Sonia Kim, Sergey Edunov, Shaoliang Nie, Sharan Narang, Sharath Raparthy, Sheng Shen, Shengyuan Wan, Shruti Bhosale, Shun Zhang, Simon Vandenhende, Soumya Batra, Spencer Whitman, Sten Sootla, Stephane Collot, Suchin Gururangan, Sydney Borodinsky, Tamar Herman, Tara Fowler, Tarek Sheasha, Thomas Georgiou, Thomas Scialom, Tobias Speckbacher, Todor Mihaylov, Tong Xiao, Ujjwal Karn, Vedanuj Goswami, Vibhor Gupta, Vignesh Ramanathan, Viktor Kerkez, Vincent Gonguet, Virginie Do, Vish Vogeti, Vítor Albiero, Vladan Petrovic, Weiwei Chu, Wenhan Xiong, Wenyin Fu, Whitney Meers, Xavier Martinet, Xiaodong Wang, Xiaofang Wang, Xiaoqing Ellen Tan, Xide Xia, Xinfeng Xie, Xuchao Jia, Xuwei Wang, Yaelle Goldschlag, Yashesh Gaur, Yasmine Babaei, Yi Wen, Yiwen Song, Yuchen Zhang, Yue Li, Yuning Mao, Zacharie Delpierre Coudert, Zheng Yan, Zhengxing Chen, Zoe Papakipos, Aaditya Singh, Aayushi Srivastava, Abha Jain, Adam Kelsey, Adam Shajnfeld, Adithya Gangidi, Adolfo Victoria, Ahuva Goldstand, Ajay Menon, Ajay Sharma, Alex Boesenberg, Alexei Baevski, Allie Feinstein, Amanda Kallet, Amit Sangani, Amos Teo, Anam Yunus, Andrei Lupu, Andres Alvarado, Andrew Caples, Andrew Gu, Andrew Ho, Andrew Poulton, Andrew Ryan, Ankit Ramchandani, Annie Dong, Annie Franco, Anuj Goyal, Aparajita Saraf, Arkabandhu Chowdhury, Ashley Gabriel, Ashwin Bharambe, Assaf Eisenman, Azadeh Yazdan, Beau James, Ben Maurer, Benjamin Leonhardi, Bernie Huang, Beth Loyd, Beto De Paola, Bhargavi Paranjape, Bing Liu, Bo Wu, Boyu Ni, Braden Hancock, Bram Wasti, Brandon Spence, Brani Stojkovic, Brian Gamido, Britt Montalvo, Carl Parker, Carly Burton, Catalina Mejia, Ce Liu, Changan Wang, Changkyu Kim, Chao Zhou, Chester Hu, Ching-Hsiang Chu, Chris Cai, Chris Tindal, Christoph Feichtenhofer, Cynthia Gao, Damon Civin, Dana Beaty, Daniel Kreymer, Daniel Li, David Adkins, David Xu, Davide Testuggine, Delia David, Devi Parikh, Diana Liskovitch, Didem Foss, Dingkang Wang, Duc Le, Dustin Holland, Edward Dowling, Eissa Jamil, Elaine Montgomery, Eleonora Presani, Emily Hahn, Emily Wood, Eric-Tuan Le, Erik Brinkman, Esteban Arcaute, Evan Dunbar, Evan Smothers, Fei Sun, Felix Kreuk, Feng Tian, Filippos Kokkinos, Firat Ozgenel, Francesco Caggioni, Frank Kanayet, Frank Seide, Gabriela Medina Florez, Gabriella Schwarz, Gada Badeer, Georgia Swee, Gil Halpern, Grant Herman, Grigory Sizov, Guangyi Zhang, Guna Lakshminarayanan, Hakan Inan, Hamid Shojanazeri, Han Zou, Hannah Wang, Hanwen Zha, Haroun Habeeb, Harrison Rudolph, Helen Suk, Henry Aspegren, Hunter Goldman, Hongyuan Zhan, Ibrahim Damlaj, Igor Molybog, Igor

Tufanov, Ilias Leontiadis, Irina-Elena Veliche, Itai Gat, Jake Weissman, James Geboski, James Kohli, Janice Lam, Japhet Asher, Jean-Baptiste Gaya, Jeff Marcus, Jeff Tang, Jennifer Chan, Jenny Zhen, Jeremy Reizenstein, Jeremy Teboul, Jessica Zhong, Jian Jin, Jingyi Yang, Joe Cummings, Jon Carvill, Jon Shepard, Jonathan McPhie, Jonathan Torres, Josh Ginsburg, Junjie Wang, Kai Wu, Kam Hou U, Karan Saxena, Kartikay Khandelwal, Katayoun Zand, Kathy Matosich, Kaushik Veeraraghavan, Kelly Michelena, Keqian Li, Kiran Jagadeesh, Kun Huang, Kunal Chawla, Kyle Huang, Lailin Chen, Lakshya Garg, Lavender A, Leandro Silva, Lee Bell, Lei Zhang, Liangpeng Guo, Licheng Yu, Liron Moshkovich, Luca Wehrstedt, Madian Khabsa, Manav Avalani, Manish Bhatt, Martynas Mankus, Matan Hasson, Matthew Lennie, Matthias Reso, Maxim Groshev, Maxim Naumov, Maya Lathi, Meghan Keneally, Miao Liu, Michael L. Seltzer, Michal Valko, Michelle Restrepo, Mihir Patel, Mik Vyatskov, Mikayel Samvelyan, Mike Clark, Mike Macey, Mike Wang, Miquel Jubert Hermoso, Mo Metanat, Mohammad Rastegari, Munish Bansal, Nandhini Santhanam, Natascha Parks, Natasha White, Navyata Bawa, Nayan Singhal, Nick Egebo, Nicolas Usunier, Nikhil Mehta, Nikolay Pavlovich Laptev, Ning Dong, Norman Cheng, Oleg Chernoguz, Olivia Hart, Omkar Salpekar, Ozlem Kalinli, Parkin Kent, Parth Parekh, Paul Saab, Pavan Balaji, Pedro Rittner, Philip Bontrager, Pierre Roux, Piotr Dollar, Polina Zvyagina, Prashant Ratanchandani, Pritish Yuvraj, Qian Liang, Rachad Alao, Rachel Rodriguez, Rafi Ayub, Raghotham Murthy, Raghu Nayani, Rahul Mitra, Rangaprabhu Parthasarathy, Raymond Li, Rebekkah Hogan, Robin Battey, Rocky Wang, Russ Howes, Ruty Rinott, Sachin Mehta, Sachin Siby, Sai Jayesh Bondu, Samyak Datta, Sara Chugh, Sara Hunt, Sargun Dhillon, Sasha Sidorov, Satadru Pan, Saurabh Mahajan, Saurabh Verma, Seiji Yamamoto, Sharadh Ramaswamy, Shaun Lindsay, Shaun Lindsay, Sheng Feng, Shenghao Lin, Shengxin Cindy Zha, Shishir Patil, Shiva Shankar, Shuqiang Zhang, Shuqiang Zhang, Sinong Wang, Sneha Agarwal, Soji Sajuyigbe, Soumith Chintala, Stephanie Max, Stephen Chen, Steve Kehoe, Steve Satterfield, Sudarshan Govindaprasad, Sumit Gupta, Summer Deng, Sungmin Cho, Sunny Virk, Suraj Subramanian, Sy Choudhury, Sydney Goldman, Tal Remez, Tamar Glaser, Tamara Best, Thilo Koehler, Thomas Robinson, Tianhe Li, Tianjun Zhang, Tim Matthews, Timothy Chou, Tzook Shaked, Varun Vontimitta, Victoria Ajayi, Victoria Montanez, Vijai Mohan, Vinay Satish Kumar, Vishal Mangla, Vlad Ionescu, Vlad Poenaru, Vlad Tiberiu Mihalescu, Vladimir Ivanov, Wei Li, Wenchen Wang, Wenwen Jiang, Wes Bouaziz, Will Constable, Xiaocheng Tang, Xiaojian Wu, Xiaolan Wang, Xilun Wu, Xinbo Gao, Yaniv Kleinman, Yanjun Chen, Ye Hu, Ye Jia, Ye Qi, Yenda Li, Yilin Zhang, Ying Zhang, Yossi Adi, Youngjin Nam, Yu, Wang, Yu Zhao, Yuchen Hao, Yundi Qian, Yunlu Li, Yuzi He, Zach Rait, Zachary DeVito, Zef Rosnbrick, Zhaoduo Wen, Zhenyu Yang, Zhiwei Zhao, and Zhiyu Ma. The llama 3 herd of models. *arXiv*, 2024. URL <https://arxiv.org/abs/2407.21783>.

Ryan Greenblatt, Carson Denison, Benjamin Wright, Fabien Roger, Monte MacDiarmid, Sam Marks, Johannes Treutlein, Tim Belonax, Jack Chen, David Duvenaud, Akbir Khan, Julian Michael, Sören Mindermann, Ethan Perez, Linda Petrini, Jonathan Uesato, Jared Kaplan, Buck Shlegeris, Samuel R. Bowman, and Evan Hubinger. Alignment faking in large language models. *arXiv*, 2024. URL <https://arxiv.org/abs/2412.14093>.

Yaru Hao, Li Dong, Furu Wei, and Ke Xu. Investigating learning dynamics of BERT fine-tuning. In Kam-Fai Wong, Kevin Knight, and Hua Wu (eds.), *Proceedings of the 1st Conference of the Asia-Pacific Chapter of the Association for Computational Linguistics and the 10th International Joint Conference on Natural Language Processing*, pp. 87–92, Suzhou, China, December 2020. Association for Computational Linguistics. doi: 10.18653/v1/2020.acl-main.11. URL <https://aclanthology.org/2020.acl-main.11/>.

Robert Huben, Hoagy Cunningham, Logan Riggs Smith, Aidan Ewart, and Lee Sharkey. Sparse autoencoders find highly interpretable features in language models. In *The Twelfth Interna-*

- tional Conference on Learning Representations*, 2024. URL <https://openreview.net/forum?id=F76bwRSLeK>.
- Samyak Jain, Robert Kirk, Ekdeep Singh Lubana, Robert P. Dick, Hidenori Tanaka, Tim Rocktäschel, Edward Grefenstette, and David Krueger. Mechanistically analyzing the effects of fine-tuning on procedurally defined tasks. In *The Twelfth International Conference on Learning Representations*, 2024. URL <https://openreview.net/forum?id=A0HKeK14N1>.
- Pegah Khayatan, Mustafa Shukor, Jayneel Parekh, and Matthieu Cord. Analyzing fine-tuning representation shift for multimodal llms steering alignment. *arXiv*, 2025. URL <https://arxiv.org/abs/2501.03012>.
- Connor Kissane, Robert Krzyzanowski, Arthur Conmy, and Neel Nanda. Open source replication of Anthropic’s crosscoder paper for model-diffing. *LessWrong*, October 2024a. URL <https://www.lesswrong.com/posts/srt6JXsRMtmqAJavD/open-source-replication-of-anthropic-s-crosscoder-paper-for>.
- Connor Kissane, robertzk, Arthur Conmy, and Neel Nanda. Base LLMs refuse too, September 2024b. URL <https://www.lesswrong.com/posts/YWo2cKJgL7Lg8xWjj/base-llms-refuse-too>.
- Olga Kovaleva, Alexey Romanov, Anna Rogers, and Anna Rumshisky. Revealing the dark secrets of BERT. In Kentaro Inui, Jing Jiang, Vincent Ng, and Xiaojun Wan (eds.), *Proceedings of the 2019 Conference on Empirical Methods in Natural Language Processing and the 9th International Joint Conference on Natural Language Processing (EMNLP-IJCNLP)*, pp. 4365–4374, Hong Kong, China, November 2019. doi: 10.18653/v1/D19-1445. URL <https://aclanthology.org/D19-1445/>.
- Andrew Lee, Xiaoyan Bai, Itamar Pres, Martin Wattenberg, Jonathan K. Kummerfeld, and Rada Mihalcea. A mechanistic understanding of alignment algorithms: A case study on DPO and toxicity. In *Proceedings of the 41st International Conference on Machine Learning, ICML’24*, 2024.
- Chak Tou Leong, Qingyu Yin, Jian Wang, and Wenjie Li. Why safeguarded ships run aground? aligned large language models’ safety mechanisms tend to be anchored in the template region. *arXiv*, 2025. URL <https://arxiv.org/abs/2502.13946>.
- Jack Lindsey, Adly Templeton, Jonathan Marcus, Thomas Conerly, Joshua Batson, and Christopher Olah. Sparse crosscoders for cross-layer features and model diffing. *Transformer Circuits Thread*, 2024. URL <https://transformer-circuits.pub/2024/crosscoders/index.html>.
- Yifan Luo, Zhennan Zhou, Meitan Wang, and Bin Dong. Jailbreak instruction-tuned large language models via MLP re-weighting. *OpenReview*, 2024. URL <https://openreview.net/forum?id=P5qCqYWD53>.
- Aleksandar Makelov, Georg Lange, and Neel Nanda. Towards principled evaluations of sparse autoencoders for interpretability and control. In *ICLR 2024 Workshop on Secure and Trustworthy Large Language Models*, 2024. URL <https://openreview.net/forum?id=MHIX9H8aYF>.
- Samuel Marks, Adam Karvonen, and Aaron Mueller. dictionary learning. https://github.com/sapmarks/dictionary_learning, 2024.
- Alexander Meinke, Bronson Schoen, Jérémy Scheurer, Mikita Balesni, Rusheb Shah, and Marius Hobbhahn. Frontier models are capable of in-context scheming. *arXiv*, 2025. URL <https://arxiv.org/abs/2412.04984>.

- Amil Merchant, Elahe Rahimtoroghi, Ellie Pavlick, and Ian Tenney. What happens to BERT embeddings during fine-tuning? In Afra Alishahi, Yonatan Belinkov, Grzegorz Chrupala, Dieuwke Hupkes, Yuval Pinter, and Hassan Sajjad (eds.), *Proceedings of the Third BlackboxNLP Workshop on Analyzing and Interpreting Neural Networks for NLP*, pp. 33–44, Online, November 2020. doi: 10.18653/v1/2020.blackboxnlp-1.4. URL <https://aclanthology.org/2020.blackboxnlp-1.4>.
- Julian Minder. Understanding the surfacing of capabilities in language models. Master’s thesis, ETH Zurich, 2024.
- Julian Minder, Kevin Du, Niklas Stoehr, Giovanni Monea, Chris Wendler, Robert West, and Ryan Cotterell. Controllable context sensitivity and the knob behind it. *arXiv preprint arXiv:2411.07404*, 2024.
- Siddharth Mishra-Sharma, Trenton Bricken, Jack Lindsey, Adam Jermyn, Jonathan Marcus, Kelley Rivoire, Christopher Olah, and Thomas Henighan. Insights on crosscoder model diffing. *Transformer Circuits Thread*, 2025. URL <https://transformer-circuits.pub/2025/crosscoder-diffing-update/index.html>.
- Marius Mosbach. Analyzing pre-trained and fine-tuned language models. In Yanai Elazar, Allyson Ettinger, Nora Kassner, Sebastian Ruder, and Noah A. Smith (eds.), *Proceedings of the Big Picture Workshop*, pp. 123–134, Singapore, December 2023. Association for Computational Linguistics. doi: 10.18653/v1/2023.bigpicture-1.10. URL <https://aclanthology.org/2023.bigpicture-1.10>.
- Aaron Mueller, Jannik Brinkmann, Millicent Li, Samuel Marks, Koyena Pal, Nikhil Prakash, Can Rager, Aruna Sankaranarayanan, Arnab Sen Sharma, Jiuding Sun, Eric Todd, David Bau, and Yonatan Belinkov. The quest for the right mediator: A history, survey, and theoretical grounding of causal interpretability. *arXiv*, 2024. URL <https://arxiv.org/abs/2408.01416>.
- Pavan Kalyan Reddy Neerudu, Subba Reddy Oota, mounika marreddy, venkateswara Rao Kagita, and Manish Gupta. On robustness of finetuned transformer-based NLP models. In *The 2023 Conference on Empirical Methods in Natural Language Processing*, 2023. URL <https://openreview.net/forum?id=YWbEDZh5ga>.
- Chris Olah, Nick Cammarata, Ludwig Schubert, Gabriel Goh, Michael Petrov, and Shan Carter. Zoom in: An introduction to circuits. *Distill*, 2020. doi: 10.23915/distill.00024.001. <https://distill.pub/2020/circuits/zoom-in>.
- OpenAI, Aaron Jaech, Adam Kalai, Adam Lerer, Adam Richardson, Ahmed El-Kishky, Aiden Low, Alec Helyar, Aleksander Madry, Alex Beutel, Alex Carney, Alex Iftimie, Alex Karpenko, Alex Tachard Passos, Alexander Neitz, Alexander Prokofiev, Alexander Wei, Allison Tam, Ally Bennett, Ananya Kumar, Andre Saraiva, Andrea Vallone, Andrew Duberstein, Andrew Kondrich, Andrey Mishchenko, Andy Applebaum, Angela Jiang, Ashvin Nair, Barret Zoph, Behrooz Ghorbani, Ben Rossen, Benjamin Sokolowsky, Boaz Barak, Bob McGrew, Borys Minaiev, Botao Hao, Bowen Baker, Brandon Houghton, Brandon McKinzie, Brydon Eastman, Camillo Lugaresi, Cary Bassin, Cary Hudson, Chak Ming Li, Charles de Bourcy, Chelsea Voss, Chen Shen, Chong Zhang, Chris Koch, Chris Orsinger, Christopher Hesse, Claudia Fischer, Clive Chan, Dan Roberts, Daniel Kappler, Daniel Levy, Daniel Selsam, David Dohan, David Farhi, David Mely, David Robinson, Dimitris Tsipras, Doug Li, Dragos Oprica, Eben Freeman, Eddie Zhang, Edmund Wong, Elizabeth Proehl, Enoch Cheung, Eric Mitchell, Eric Wallace, Erik Ritter, Evan Mays, Fan Wang, Felipe Petroski Such, Filippo Raso, Florencia Leoni, Foivos Tsimpourlas, Francis Song, Fred von Lohmann, Freddie Sulit, Geoff Salmon, Giambattista Parascandolo, Gildas Chabot, Grace Zhao, Greg Brockman, Guillaume Leclerc, Hadi Salman, Haiming Bao, Hao Sheng, Hart Andrin,

- Hessam Bagherinezhad, Hongyu Ren, Hunter Lightman, Hyung Won Chung, Ian Kivlichan, Ian O’Connell, Ian Osband, Ignasi Clavera Gilaberte, Ilge Akkaya, Ilya Kostrikov, Ilya Sutskever, Irina Kofman, Jakub Pachocki, James Lennon, Jason Wei, Jean Harb, Jerry Twore, Jiacheng Feng, Jiahui Yu, Jiayi Weng, Jie Tang, Jieqi Yu, Joaquin Quiñero Candela, Joe Palermo, Joel Parish, Johannes Heidecke, John Hallman, John Rizzo, Jonathan Gordon, Jonathan Uesato, Jonathan Ward, Joost Huizinga, Julie Wang, Kai Chen, Kai Xiao, Karan Singhal, Karina Nguyen, Karl Cobbe, Katy Shi, Kayla Wood, Kendra Rimbach, Keren Gu-Lemberg, Kevin Liu, Kevin Lu, Kevin Stone, Kevin Yu, Lama Ahmad, Lauren Yang, Leo Liu, Leon Maksin, Leyton Ho, Liam Fedus, Lilian Weng, Linden Li, Lindsay McCallum, Lindsey Held, Lorenz Kuhn, Lukas Kondraciuk, Lukasz Kaiser, Luke Metz, Madelaine Boyd, Maja Trebacz, Manas Joglekar, Mark Chen, Marko Tintor, Mason Meyer, Matt Jones, Matt Kaufer, Max Schwarzer, Meghan Shah, Mehmet Yatbaz, Melody Y. Guan, Mengyuan Xu, Mengyuan Yan, Mia Glaese, Mianna Chen, Michael Lampe, Michael Malek, Michele Wang, Michelle Fradin, Mike McClay, Mikhail Pavlov, Miles Wang, Mingxuan Wang, Mira Murati, Mo Bavarian, Mostafa Rohaninejad, Nat McAleese, Neil Chowdhury, Neil Chowdhury, Nick Ryder, Nikolas Tezak, Noam Brown, Ofir Nachum, Oleg Boiko, Oleg Murk, Olivia Watkins, Patrick Chao, Paul Ashbourne, Pavel Izmailov, Peter Zhokhov, Rachel Dias, Rahul Arora, Randall Lin, Rapha Gontijo Lopes, Raz Gaon, Reah Miyara, Reimar Leike, Renny Hwang, Rhythm Garg, Robin Brown, Roshan James, Rui Shu, Ryan Cheu, Ryan Greene, Saachi Jain, Sam Altman, Sam Toizer, Sam Toyer, Samuel Miserendino, Sandhini Agarwal, Santiago Hernandez, Sasha Baker, Scott McKinney, Scottie Yan, Shengjia Zhao, Shengli Hu, Shibani Santurkar, Shraman Ray Chaudhuri, Shuyuan Zhang, Siyuan Fu, Spencer Papay, Steph Lin, Suchir Balaji, Suvansh Sanjeev, Szymon Sidor, Tal Broda, Aidan Clark, Tao Wang, Taylor Gordon, Ted Sanders, Tejal Patwardhan, Thibault Sottiaux, Thomas Degry, Thomas Dimson, Tianhao Zheng, Timur Garipov, Tom Stasi, Trapit Bansal, Trevor Creech, Troy Peterson, Tyna Eloundou, Valerie Qi, Vineet Kosaraju, Vinnie Monaco, Vitchyr Pong, Vlad Fomenko, Weiyi Zheng, Wenda Zhou, Wes McCabe, Wojciech Zaremba, Yann Dubois, Yinghai Lu, Yining Chen, Young Cha, Yu Bai, Yuchen He, Yuchen Zhang, Yunyun Wang, Zheng Shao, and Zhuohan Li. Openai ol system card. *arXiv*, 2024. URL <https://arxiv.org/abs/2412.16720>.
- Gonçalo Paulo, Alex Mallen, Caden Juang, and Nora Belrose. Automatically interpreting millions of features in large language models. *arXiv*, 2024. URL <https://arxiv.org/abs/2410.13928>.
- Guilherme Penedo, Quentin Malartic, Daniel Hesslow, Ruxandra Cojocaru, Alessandro Cappelli, Hamza Alobeidli, Baptiste Pannier, Ebtesam Almazrouei, and Julien Launay. The refinedweb dataset for falcon llm: Outperforming curated corpora with web data, and web data only. *arXiv*, 2023. URL <https://arxiv.org/abs/2306.01116>.
- Jason Phang, Haokun Liu, and Samuel R. Bowman. Fine-tuned transformers show clusters of similar representations across layers. *arXiv*, 2021. URL <https://arxiv.org/abs/2109.08406>.
- Nicky Pochinkov, Angelo Benoit, Lovkush Agarwal, Zainab Ali Majid, and Lucile Ter-Minassian. Extracting paragraphs from LLM token activations. In *MINT: Foundation Model Interventions*, 2024. URL <https://openreview.net/forum?id=4b675AHcqq>.
- Nikhil Prakash, Tamar Rott Shaham, Tal Haklay, Yonatan Belinkov, and David Bau. Fine-tuning enhances existing mechanisms: A case study on entity tracking. In *The Twelfth International Conference on Learning Representations*, 2024. URL <https://openreview.net/forum?id=8sKcAW0f2D>.
- Xiangyu Qi, Ashwinee Panda, Kaifeng Lyu, Xiao Ma, Subhrajit Roy, Ahmad Beirami, Prateek Mittal, and Peter Henderson. Safety alignment should be made more than just a few tokens deep. *arXiv*, 2024. URL <https://arxiv.org/abs/2406.05946>.

- Evani Radiya-Dixit and Xin Wang. How fine can fine-tuning be? Learning efficient language models. In Silvia Chiappa and Roberto Calandra (eds.), *Proceedings of the Twenty Third International Conference on Artificial Intelligence and Statistics*, volume 108 of *Proceedings of Machine Learning Research*, pp. 2435–2443, 26–28 Aug 2020. URL <https://proceedings.mlr.press/v108/radiya-dixit20a.html>.
- Senthooran Rajamanoharan, Arthur Conmy, Lewis Smith, Tom Lieberum, Vikrant Varma, Janos Kramar, Rohin Shah, and Neel Nanda. Improving sparse decomposition of language model activations with gated sparse autoencoders. In *The Thirty-eighth Annual Conference on Neural Information Processing Systems*, 2024. URL <https://openreview.net/forum?id=zLBlin2zvW>.
- Nils Reimers and Iryna Gurevych. Sentence-BERT: Sentence embeddings using Siamese BERT-networks. In Kentaro Inui, Jing Jiang, Vincent Ng, and Xiaojun Wan (eds.), *Proceedings of the 2019 Conference on Empirical Methods in Natural Language Processing and the 9th International Joint Conference on Natural Language Processing (EMNLP-IJCNLP)*, pp. 3982–3992, Hong Kong, China, November 2019. doi: 10.18653/v1/D19-1410. URL <https://aclanthology.org/D19-1410/>.
- Morgane Riviere, Shreya Pathak, Pier Giuseppe Sessa, Cassidy Hardin, Surya Bhupatiraju, Léonard Hussenot, Thomas Mesnard, Bobak Shahriari, Alexandre Ramé, et al. Gemma 2: Improving open language models at a practical size. *arXiv preprint arXiv:2408.00118*, 2024.
- Alok N. Shah, Keshav Ramji, Khush Gupta, and Vedant Gaur. Investigating language model dynamics using meta-tokens. In *Second NeurIPS Workshop on Attributing Model Behavior at Scale*, 2024. URL <https://openreview.net/forum?id=pFjEYaZtZl>.
- Lee Sharkey, Bilal Chughtai, Joshua Batson, Jack Lindsey, Jeff Wu, Lucius Bushnaq, Nicholas Goldowsky-Dill, Stefan Heimersheim, Alejandro Ortega, Joseph Bloom, Stella Biderman, Adria Garriga-Alonso, Arthur Conmy, Neel Nanda, Jessica Rumbelow, Martin Wattenberg, Nandi Schoots, Joseph Miller, Eric J. Michaud, Stephen Casper, Max Tegmark, William Saunders, David Bau, Eric Todd, Atticus Geiger, Mor Geva, Jesse Hoogland, Daniel Murfet, and Tom McGrath. Open problems in mechanistic interpretability. *arXiv*, 2025. URL <https://arxiv.org/abs/2501.16496>.
- Mrinank Sharma, Meg Tong, Tomasz Korbak, David Duvenaud, Amanda Askill, Samuel R. Bowman, Newton Cheng, Esin Durmus, Zac Hatfield-Dodds, Scott R. Johnston, Shauna Kravec, Timothy Maxwell, Sam McCandlish, Kamal Ndousse, Oliver Rausch, Nicholas Schiefer, Da Yan, Miranda Zhang, and Ethan Perez. Towards understanding sycophancy in language models. *arXiv*, 2023. URL <https://arxiv.org/abs/2310.13548>.
- Adly Templeton, Tom Conerly, Jonathan Marcus, Jack Lindsey, Trenton Bricken, Brian Chen, Adam Pearce, Craig Citro, Emmanuel Ameisen, Andy Jones, Hoagy Cunningham, Nicholas L Turner, Callum McDougall, Monte MacDiarmid, C. Daniel Freeman, Theodore R. Sumers, Edward Rees, Joshua Batson, Adam Jermyn, Shan Carter, Chris Olah, and Tom Henighan. Scaling monosemanticity: Extracting interpretable features from claude 3 sonnet. *Transformer Circuits Thread*, 2024. URL <https://transformer-circuits.pub/2024/scaling-monosemanticity/index.html>.
- Harrish Thasarathan, Julian Forsyth, Thomas Fel, Matthew Kowal, and Konstantinos Derpanis. Universal sparse autoencoders: Interpretable cross-model concept alignment. *arXiv*, 2025. URL <https://arxiv.org/abs/2502.03714>.

- Curt Tigges, Oskar John Hollinsworth, Atticus Geiger, and Neel Nanda. Language models linearly represent sentiment. In Yonatan Belinkov, Najoung Kim, Jaap Jumelet, Hosein Mohebbi, Aaron Mueller, and Hanjie Chen (eds.), *Proceedings of the 7th BlackboxNLP Workshop: Analyzing and Interpreting Neural Networks for NLP*, pp. 58–87, Miami, Florida, US, November 2024. doi: 10.18653/v1/2024.blackboxnlp-1.5. URL <https://aclanthology.org/2024.blackboxnlp-1.5/>.
- Francisco Vargas and Ryan Cotterell. Exploring the linear subspace hypothesis in gender bias mitigation. In Bonnie Webber, Trevor Cohn, Yulan He, and Yang Liu (eds.), *Proceedings of the 2020 Conference on Empirical Methods in Natural Language Processing (EMNLP)*, pp. 2902–2913, Online, November 2020. Association for Computational Linguistics. doi: 10.18653/v1/2020.emnlp-main.232. URL <https://aclanthology.org/2020.emnlp-main.232/>.
- Kevin Ro Wang, Alexandre Variengien, Arthur Conmy, Buck Shlegeris, and Jacob Steinhardt. Interpretability in the wild: a circuit for indirect object identification in GPT-2 small. In *The Eleventh International Conference on Learning Representations, 2023a*. URL <https://openreview.net/forum?id=NpsVSN6o4u1>.
- Yihan Wang, Andrew Bai, Nanyun Peng, and Cho-Jui Hsieh. On the loss of context-awareness in general instruction finetuning. *OpenReview*, 2024. URL <https://openreview.net/forum?id=eDns1TIWSt>.
- Zihao Wang, Lin Gui, Jeffrey Negrea, and Victor Veitch. Concept algebra for (score-based) text-controlled generative models. In A. Oh, T. Naumann, A. Globerson, K. Saenko, M. Hardt, and S. Levine (eds.), *Advances in Neural Information Processing Systems*, volume 36, pp. 35331–35349. Curran Associates, Inc., 2023b. URL https://proceedings.neurips.cc/paper_files/paper/2023/file/6f125214c86439d107ccb58e549e828f-Paper-Conference.pdf.
- Benjamin Wright and Lee Sharkey. Addressing feature suppression in SAEs. *LessWrong*, 2024. URL <https://www.lesswrong.com/posts/3JuSjTzYmzaSeTxKk/addressing-feature-suppression-in-saes>.
- Xuansheng Wu, Wenlin Yao, Jianshu Chen, Xiaoman Pan, Xiaoyang Wang, Ninghao Liu, and Dong Yu. From language modeling to instruction following: Understanding the behavior shift in LLMs after instruction tuning. In Kevin Duh, Helena Gomez, and Steven Bethard (eds.), *Proceedings of the 2024 Conference of the North American Chapter of the Association for Computational Linguistics: Human Language Technologies (Volume 1: Long Papers)*, pp. 2341–2369, Mexico City, Mexico, June 2024. doi: 10.18653/v1/2024.naacl-long.130. URL <https://aclanthology.org/2024.naacl-long.130>.
- Zeyu Yun, Yubei Chen, Bruno Olshausen, and Yann LeCun. Transformer visualization via dictionary learning: contextualized embedding as a linear superposition of transformer factors. In Eneko Agirre, Marianna Apidianaki, and Ivan Vulić (eds.), *Proceedings of Deep Learning Inside Out (DeeLIO): The 2nd Workshop on Knowledge Extraction and Integration for Deep Learning Architectures*, pp. 1–10, Online, June 2021. doi: 10.18653/v1/2021.deelio-1.1. URL <https://aclanthology.org/2021.deelio-1.1/>.
- Lianmin Zheng, Wei-Lin Chiang, Ying Sheng, Tianle Li, Siyuan Zhuang, Zhanghao Wu, Yonghao Zhuang, Zhuohan Li, Zi Lin, Eric P. Xing, Joseph E. Gonzalez, Ion Stoica, and Hao Zhang. Lmsys-chat-1m: A large-scale real-world llm conversation dataset. *arXiv*, 2024. URL <https://arxiv.org/abs/2309.11998>.

A APPENDIX

A.1 COMPARING SPARSITY LOSSES: CROSSCODER VS. STACKED SAE

An L1 crosscoder can be viewed as an SAE operating on stacked activations, where the encoder and decoder vectors are similarly stacked:

$$\mathbf{h}(x) = [\mathbf{h}^{\text{base}}(x), \mathbf{h}^{\text{chat}}(x)] \in \mathbb{R}^{2d} \quad (17)$$

$$\mathbf{e}_j = [\mathbf{e}_j^{\text{base}}, \mathbf{e}_j^{\text{chat}}] \in \mathbb{R}^{2d} \quad (18)$$

$$\mathbf{d}_j = [\mathbf{d}_j^{\text{base}}, \mathbf{d}_j^{\text{chat}}] \in \mathbb{R}^{2d} \quad (19)$$

$$\mathbf{b}^{\text{dec}} = [\mathbf{b}^{\text{dec,base}}, \mathbf{b}^{\text{dec,chat}}] \quad (20)$$

The reconstruction remains equivalent because

$$f_j(x) = \text{ReLU}(\mathbf{e}_j \mathbf{h} + b_j^{\text{enc}}) \quad (21)$$

$$\begin{aligned} &= \text{ReLU}(\mathbf{e}_j^{\text{base}} \mathbf{h}^{\text{base}}(x) + \\ &\quad \mathbf{e}_j^{\text{chat}} \mathbf{h}^{\text{chat}}(x) + b_j^{\text{enc}}) \end{aligned} \quad (22)$$

and hence,

$$[\tilde{\mathbf{h}}^{\text{base}}(x), \tilde{\mathbf{h}}^{\text{chat}}(x)] = \sum_j f_j(x) \mathbf{d}_j + \mathbf{b}^{\text{dec}} \quad (23)$$

However, the key difference arises in the sparsity loss. For the crosscoder, the sparsity loss is given by:

$$\begin{aligned} L_{\text{sparsity}}^{\text{crosscoder}}(x) &= \sum_j f_j(x) \left(\sqrt{\sum_{i=1}^d (\mathbf{d}_{j,i}^{\text{chat}})^2} \right. \\ &\quad \left. + \sqrt{\sum_{i=1}^d (\mathbf{d}_{j,i}^{\text{base}})^2} \right) \end{aligned} \quad (24)$$

For a stacked SAE, it is:

$$\begin{aligned} L_{\text{sparsity}}^{\text{SAE}}(x) &= \sum_j f_j(x) \sqrt{\sum_{i=1}^{2d} (\mathbf{d}_{j,i})^2} \\ &= \sum_j f_j(x) \sqrt{\sum_{i=1}^d (\mathbf{d}_{j,i}^{\text{base}})^2 + \sum_{i=1}^d (\mathbf{d}_{j,i}^{\text{chat}})^2} \end{aligned} \quad (25)$$

The difference between $\sqrt{x+y}$ and $\sqrt{x} + \sqrt{y}$ introduces an inductive bias in the crosscoder that encourages the norm of one decoder (often the base decoder) to approach zero when the corresponding latent is only informative in one model.

Figure 10 displays a heatmap of the functions $\sqrt{x^2 + y^2}$ and $\sqrt{x^2} + \sqrt{y^2}$ along with their negative gradients, as visualized by the arrows. One can observe that for the crosscoder sparsity variant $\sqrt{x^2} + \sqrt{y^2}$ the gradient encourages the norm of one of the decoders to approach zero much more quickly compared to the SAE's $\sqrt{x^2 + y^2}$.

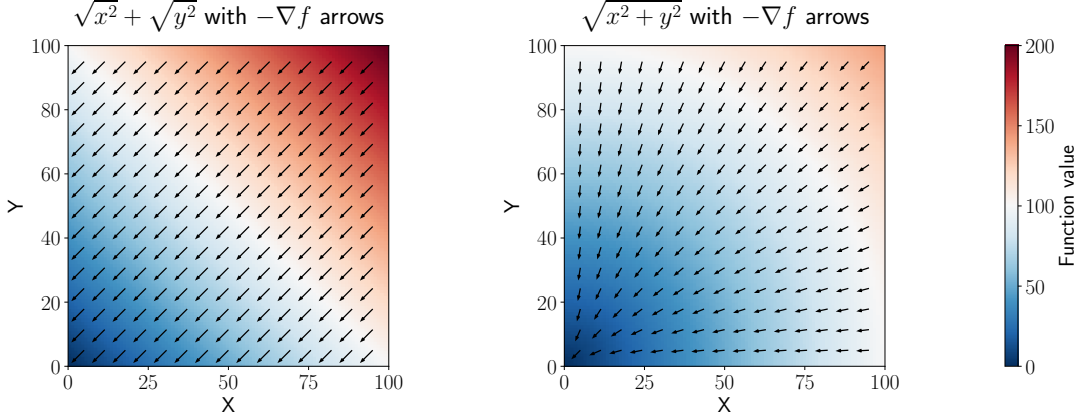


Figure 10: Heatmap comparing the two functions $\sqrt{x^2 + y^2}$ and $\sqrt{x^2} + \sqrt{y^2}$ along with their negative gradients.

A.2 DETAILED SETUP FOR ACTIVATION DIVERGENCE

In order to compute the activation divergence we compute for each pairs $p = (i, j)$, we first compute the max pair activation A_p on the training set D_{train} (containing data from LMSYS and FineWeb)

$$A_p = \max(A_i, A_j)$$

$$A_i = \max\{f_i(x)(\|\mathbf{d}_i^{\text{chat}}\| + \|\mathbf{d}_i^{\text{base}}\|), x \in D_{\text{train}}\}$$

Then the divergence Div_p is computed as follow

$$\text{Div}_p = \frac{\text{Single}_p}{\text{High}_p}$$

$$\text{Single}_p = \#\text{single}_i + \#\text{single}_j$$

$$\text{High}_p = \#(\text{high}_i \cup \text{high}_j)$$

where $\#\text{single}_i$ is the set of input $x \in D_{\text{val}}$ where i has a high activation but not j and high_i is the total number of high activations computed as follows:

$$\text{only}_i = \{x \in D_{\text{val}}, f_i(x) > 0.7A_p$$

$$\quad \wedge f_j(x) < 0.3A_p\}$$

$$\text{high}_i = \{x \in D_{\text{val}}, f_i(x) > 0.7A_p\}$$

A.3 ILLUSTRATIVE EXAMPLE OF LATENT DECOUPLING

To illustrate the phenomenon of Latent Decoupling we choose the oversimplified case where $f_{\text{b-excl}}(x) = f_{\text{c-excl}}(x) = 0$. Let us consider a latent j with $f_j(x) = \alpha$. On the other hand, let there be two other latents p and q with

$$\mathbf{d}_p^{\text{base}} = \mathbf{d}_j^{\text{base}}, \quad \mathbf{d}_p^{\text{chat}} = \mathbf{0}$$

$$\mathbf{d}_q^{\text{base}} = \mathbf{0}, \quad \mathbf{d}_q^{\text{chat}} = \mathbf{d}_j^{\text{chat}}$$

and $f_p(x) = f_q(x) = \alpha$. Clearly, the reconstruction is the same in both cases since $\alpha \mathbf{d}_j^{\text{base}} = \alpha \mathbf{d}_q^{\text{base}} + \alpha \mathbf{d}_q^{\text{chat}}$ and $\alpha \mathbf{d}_j^{\text{chat}} = \alpha \mathbf{d}_q^{\text{chat}} + \alpha \mathbf{d}_q^{\text{chat}}$. Further, the L1 regularization term is the same since

$$\alpha (\|\mathbf{d}_j^{\text{base}}\|_2 + \|\mathbf{d}_j^{\text{chat}}\|_2) = \quad (26)$$

$$\begin{aligned} & \alpha (\|\mathbf{d}_p^{\text{base}}\|_2 + \|\mathbf{d}_p^{\text{chat}}\|_2) \\ & + \alpha (\|\mathbf{d}_q^{\text{base}}\|_2 + \|\mathbf{d}_q^{\text{chat}}\|_2) \\ & = \alpha (\|\mathbf{d}_p^{\text{base}}\|_2 + 0) + \alpha (0 + \|\mathbf{d}_q^{\text{chat}}\|_2) \end{aligned} \quad (27)$$

Hence both solutions achieve the exact same loss.

A.4 CLOSED FORM SOLUTION FOR LATENT SCALING

Consider a latent j with decoder vector \mathbf{d} . Our goal is to find the optimal scaling factor β that minimizes the squared reconstruction error:

$$\operatorname{argmin}_{\beta} \sum_{i=0}^n \|\beta f(x_i) \mathbf{d} - \mathbf{y}\|_2^2 \quad (28)$$

To solve this optimization problem efficiently, we reformulate it in matrix form. Let $\mathbf{Y} \in \mathbb{R}^{n \times d}$ be the stacked data matrix and $\mathbf{f} \in \mathbb{R}^n$ be the vector of latent activations for latent j across all datapoints. The objective can then be expressed using the Frobenius norm of the residual matrix $\mathbf{R} = \beta \mathbf{f} \mathbf{d}^T - \mathbf{Y}$, where $\mathbf{f} \mathbf{d}^T \in \mathbb{R}^{n \times d}$ represents the outer product of the latent activation vector and decoder vector. Our minimization problem becomes:

$$\|\mathbf{R}\|_F^2 = \|\beta \mathbf{f} \mathbf{d}^T - \mathbf{Y}\|_F^2 \quad (29)$$

$$= \operatorname{Tr} [(\beta \mathbf{f} \mathbf{d}^T - \mathbf{Y})^\top (\beta \mathbf{f} \mathbf{d}^T - \mathbf{Y})] \quad (30)$$

$$\begin{aligned} & = \operatorname{Tr} [\mathbf{Y}^\top \mathbf{Y}] - 2\beta \operatorname{Tr} [\mathbf{Y}^\top \mathbf{f} \mathbf{d}^T] \\ & \quad + \beta^2 \operatorname{Tr} [(\mathbf{f} \mathbf{d}^T)^\top \mathbf{f} \mathbf{d}^T] \end{aligned} \quad (31)$$

Using trace properties, we get:

$$\operatorname{Tr} [\mathbf{Y}^\top \mathbf{f} \mathbf{d}^T] = \mathbf{d}^\top (\mathbf{Y}^\top \mathbf{f}) \quad (32)$$

$$\operatorname{Tr} [(\mathbf{f} \mathbf{d}^T)^\top \mathbf{f} \mathbf{d}^T] = \|\mathbf{f}\|_2^2 \|\mathbf{d}\|_2^2 \quad (33)$$

Taking the derivative with respect to β and setting it to zero:

$$\frac{\delta}{\delta \beta} \|\mathbf{R}\|_F^2 = -2\mathbf{d}^\top (\mathbf{Y}^\top \mathbf{f}) + 2\beta \|\mathbf{f}\|_2^2 \|\mathbf{d}\|_2^2 = 0 \quad (34)$$

This yields the closed form solution:

$$\beta = \frac{\mathbf{d}^\top (\mathbf{Y}^\top \mathbf{f})}{\|\mathbf{f}\|_2^2 \|\mathbf{d}\|_2^2} \quad (35)$$

A.5 DETAILED SETUP FOR LATENT SCALING

We specify the exact target vectors \mathbf{y} used in Equation (12) for computing the different β values. To measure how well latent j explains the reconstruction *error*, we exclude latent j from the reconstruction. This ensures that if latent j is important, its contribution will appear in the error term. For chat-only latents, we expect distinct behavior in each model: no contribution in the base model ($\beta_j^{\varepsilon, \text{base}} \approx 0$) but strong contribution in the chat model ($\beta_j^{\varepsilon, \text{chat}} \approx 1$), resulting in $\nu_j^{\varepsilon} \approx 0$. In contrast, *shared* latents should have similar contributions in both models, resulting in approximately equal values for $\beta_j^{\varepsilon, \text{base}}$ and $\beta_j^{\varepsilon, \text{chat}}$ and consequently $\nu_j^{\varepsilon} \approx 1$.

$$\beta_j^{\varepsilon, \text{base}} : \mathbf{y}_i = \mathbf{h}^{\text{base}}(x_i) - \sum_{k, k \neq j} f_k(x_i) \mathbf{d}_k^{\text{base}} + \mathbf{b}^{\text{dec, base}} \quad (36)$$

$$\beta_j^{\varepsilon, \text{chat}} : \mathbf{y}_i = \mathbf{h}^{\text{chat}}(x_i) - \sum_{k, k \neq j} f_k(x_i) \mathbf{d}_k^{\text{chat}} + \mathbf{b}^{\text{dec, chat}} \quad (37)$$

To measure how well a latent j explains the *reconstruction*, we simply use

$$\beta_j^{\varepsilon, \text{base}} : \mathbf{y}_i = \mathbf{h}^{\text{base}}(x_i) \quad (38)$$

$$\beta_j^{\varepsilon, \text{chat}} : \mathbf{y}_i = \mathbf{h}^{\text{chat}}(x_i) \quad (39)$$

In a similar manner, we expect the fraction ν_j^r to be low for chat-only latents and around 1 for *shared* latents.

A.6 ADDITIONAL ANALYSIS FOR LATENT SCALING

Figure 11a and Figure 11b analyze the relationship between our scaling metrics (ν^{ε} and ν^r) and the actual improvement in reconstruction quality in the L1 crosscoder. For each latent, we compute the MSE improvement as:

$$\text{MSEImprovement} = \frac{\text{MSE}_{\text{original}} - \text{MSE}_{\text{scaled}}}{\text{MSE}_{\text{original}}}$$

where $\text{MSE}_{\text{scaled}}$ is measured after applying our latent scaling technique. We then examine the ratio of MSE improvements between the base and chat models, analogous to our ν metrics. The strong correlation between the ν values and MSE improvement ratios validates that our scaling approach captures meaningful differences in how latents contribute to reconstruction in each model.

In Figure 12, we analyze the latent scaling technique by examining its relationship with the Δ_{norm} score. Specifically, we identify the 100 latents with the lowest ν^{ε} values and analyze their rankings according to the Δ_{norm} metric. As shown in Figure 12, there is limited correlation between the two measures - simply using a lower NormDiff threshold to identify *chat-only* latents produces substantially different results from our latent scaling approach.

A.7 CAUSALITY EXPERIMENTS ON LMSYS-CHAT

In Figure 13 we repeat the causality experiments from Section 3.1.2 for the L1 crosscoder on 700'000 tokens from the LMSYS-CHAT dataset, that the crosscoder was trained on. Note that while this dataset is much larger, the model responses are not generated by the Gemma 2 2b it model, and hence the model answers are out of distribution for this model. Since this dataset is much larger, the confidence intervals are much smaller. The results are qualitatively similar to the ones on the generated dataset in the main paper.

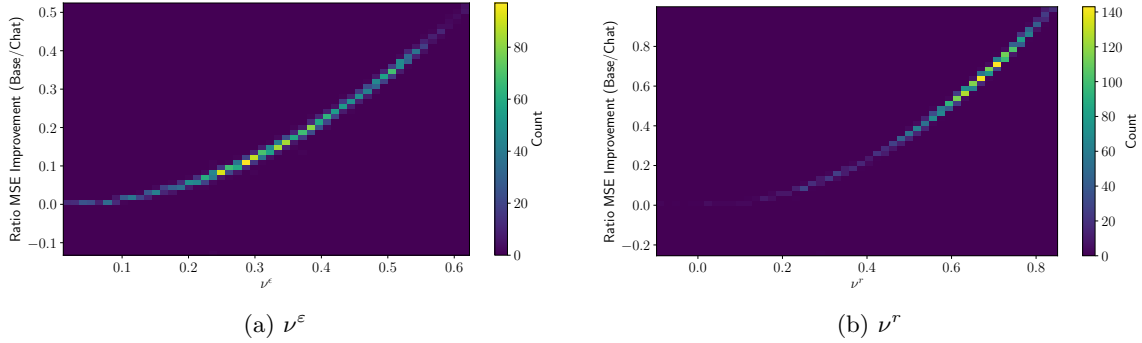


Figure 11: Comparison of the ratio of MSE improvement compared to the value of ν^ϵ and ν^r .

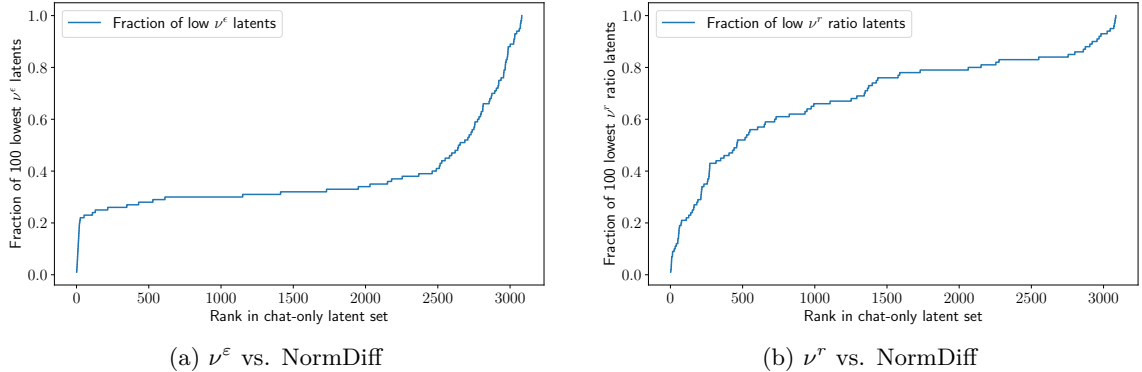


Figure 12: Comparison of latent rankings between ν and NormDiff scores. The lines shows the fraction of the 100 latents with the lowest ν values (x -axis) that have a rank lower than the given rank under the NormDiff score (y -axis).

A.8 AUTOINTERPRETABILITY DETAILS

We automatically interpret the identified latents using the pipeline from Paulo et al. (2024). To explain the latents, we provide ten activating examples from each activation tercile to Llama 3.3 70B (Grattafiori et al., 2024). Latents are scored using a modified detection metric from Paulo et al. (2024). We provide ten new activating examples from each tercile. Rather than comparing activation examples against randomly selected non-activating examples, we use semantically similar non-activating examples identified through Sentence BERT embedding similarity (Reimers & Gurevych, 2019) using the *all-MiniLM-L6-v2* model. To find these similar examples, we join all activating examples into a single string and embed it, then compute similarity scores against embeddings for each window of tokens to identify the most semantically related non-activating examples. This is a strictly harder task than scoring activation examples against a random set of non-activating examples.

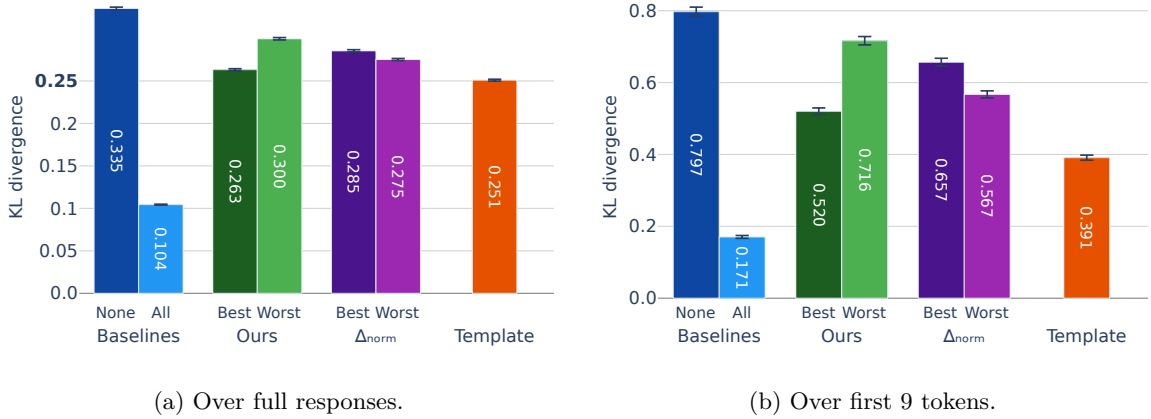


Figure 13: Comparison of KL divergence between different approximations of chat model activations on the LMSYS-CHAT dataset. We establish baselines by replacing either *None* or *All* of the latents. We then evaluate our Latent Scaling metric (*Ours*) against the relative norm difference (Δ_{norm}) by comparing the effects of replacing the top and bottom 50% of latents ranked by each metric (*Best* vs *Worst*). Additionally, we measure the impact of replacing activations only on template tokens (*Template*). We show the 95% confidence intervals for all measurements. Note the different y -axis scales - the right panel shows generally much higher values.

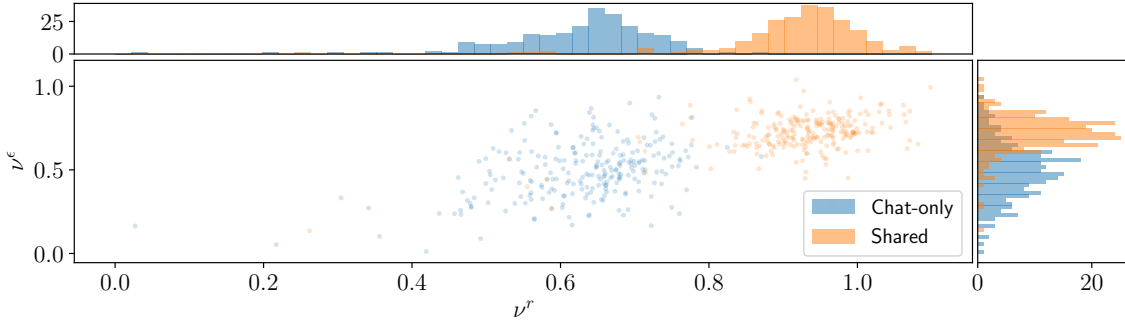


Figure 14: The x -axis is the reconstruction ratio ν^r and the y -axis is the error ratio ν^ϵ . High values on the x -axis with significant overlap with the *shared* distribution indicate Latent Decoupling. High values on the y -axis indicate Complete Shrinkage. We zoom on the ν range between 0 and 1.1.

A.9 REPRODUCING RESULTS ON INDEPENDENTLY TRAINED L1 CROSSCODER

We validate our findings by analyzing a crosscoder independently trained by Kissane et al. (2024a) on the same models and layer than ours. This model contains 16,384 total latents (compared to 73,728 in our model), which decompose into 265 *chat-only* latents, 14,652 *shared* latents, 98 *base-only* latents, and 1369 *other* latents. Figure 14 shows the reconstruction ratio ν^r and error ratio ν^ϵ for all latents, revealing patterns consistent with our previous findings in Figure 2. The overlap between *chat-only* and *shared* latents remains similar - 17.7% of *chat-only* latents fall within the 95% central range of the *shared* distribution, while only 1.1% lie within the 50% central range. We observe even

higher ν^ε values for *chat-only* latents, suggesting that quite a lot of the *chat-only* latents suffer from Complete Shrinkage. Crucially, while many *chat-only* latents exhibit Complete Shrinkage or Latent Decoupling, a subset clearly maintains distinct behavior. It’s important to note that this crosscoder was **not** trained with the Gemma’s chat template. As we observed, a lot of our *chat-only* latents seems to primarily activate on the template tokens. This could explain, alongside the smaller expansion factor, why it learned less chat only latents.

A.10 TRAINING DETAILS

We trained both crosscoders with the following setup:

- **Base Model:** Gemma 2 2B.
- **Chat Model:** Gemma 2 2B it.
- **Layer used:** 13 (of 25).
- **Initialization:**
 - Decoder initialized as the transpose of the encoder weights.
 - Encoder and decoder for both models are paired with the same initial weights.
 - **Training Data:** 100M tokens from Fineweb (web data) (Penedo et al., 2023) and lmsys-chat (chat data) (Zheng et al., 2024), respectively.

Refer to Table 2 and Table 3 for the training details. We use the tools *nnsight* (Fiotto-Kaufman et al., 2024) and *dictionary learning* (Marks et al., 2024) to train the crosscoder. The following summary table shows the training details:

Epoch	μ	LR	Split	FVE (Base)	FVE (Chat)	Dead	Total FVE	L0
1	$4e-2$	$1e-4$	Train	81.5%	82.9%	-	82.3%	112.3
			Val	83.8%	85.2%	7.8%	84.6%	112.5
2	$4.1e-2$	$1e-4$	Train	79.6%	80.7%	-	80.3%	101.7
			Val	83.6%	84.9%	8.1%	84.4%	101.0

Table 2: **L1 crosscoder training statistics.** FVE stands for Fraction of Variance Explained. LR stands for Learning Rate. The L1 regularization parameter μ was slightly increased in the second epoch to improve sparsity, resulting in lower L0 values. We present statistics for both epochs to illustrate this progression.

Epochs	k	LR	Split	FVE (Base)	FVE (Chat)	Dead	Total FVE	L0
2	100	$1e-4$	Train	86.2%	86.9%	-	86.6%	100
			Val	88.1%	87.0%	12.0%	87.6%	99.48

Table 3: **BatchTopK crosscoder training statistics.** FVE stands for Fraction of Variance Explained. LR stands for Learning Rate.

A.11 ADDITIONAL STATISTICS ON THE CROSSCODERS

In this section, we present additional statistics for both the L1 and BatchTopK crosscoders, focusing on the distribution of cosine similarities between decoder latents, latent activation frequencies and the number of *chat-only* latents mainly activating on template tokens.

Cosine similarity between decoder latents. Figure 15 shows the distribution of cosine similarity between the base and chat model decoder latents for both crosscoders. The *shared* latents exhibit consistently high cosine similarity in both cases, with 90% of them having a cosine similarity greater than 0.9 in the L1 crosscoder and 61% in the BatchTopK crosscoder. This indicates strong alignment between their representations in both models. Since the norm of one of the two decoder vectors is ≈ 0 for *base-only* and *chat-only*, these values are less informative.

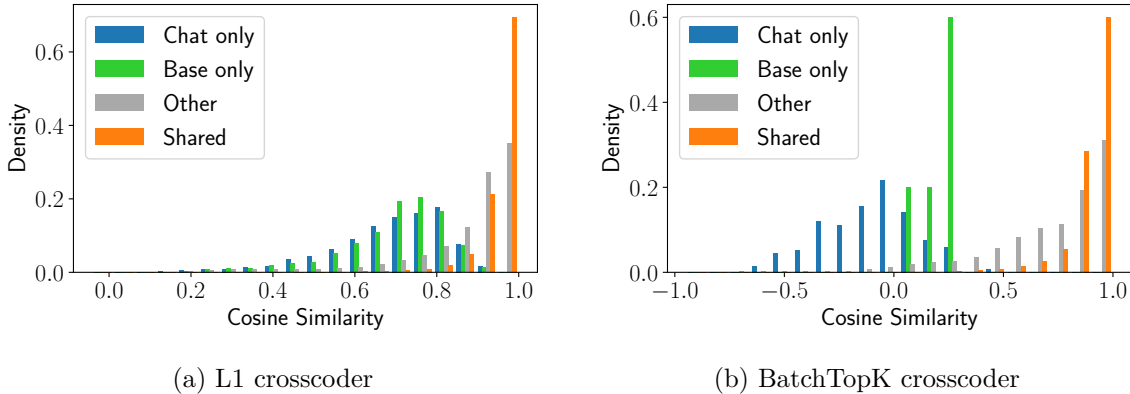


Figure 15: Distribution of cosine similarity between base and chat model decoder latents. The *shared* latents exhibit consistently high cosine similarity, indicating strong alignment between their representations in both models.

Latent activation frequencies. Figure 16 displays the latent activation frequencies for the different latent groups in both crosscoders. Similarly to (Mishra-Sharma et al., 2025), we find that *shared* latents have lower latent activation frequencies than model-specific *base-only* and *chat-only* latents. Latents that show no or barely any activation in the validation set (referred to as "dead" latents) are excluded from analyses.

Correlation with ν metrics. We observe a high Spearman correlation between our metrics and latent activation frequency in the L1 crosscoder, especially for ν^ϵ ($\nu^r : 0.458$ and $\nu^\epsilon : 0.83$ where $p < 0.05$)¹⁰. We observe no such correlation in the BatchTopK crosscoder. Mishra-Sharma et al. (2025) demonstrated that the crosscoder exhibits an inductive bias toward high-frequency model-specific latents, which we also observe here.

Template token activation percentage. Figure 17 shows the histogram of metrics ν^ϵ and ν^r across all *chat-only* latents in both crosscoders. We observe that most latents with low ν^ϵ and ν^r values predominantly activate on template tokens.

¹⁰Pearson correlation shows less correlation for ν^r ($\nu^r : -0.02$ and $\nu^\epsilon : 0.55$) since the relationship is non-linear.

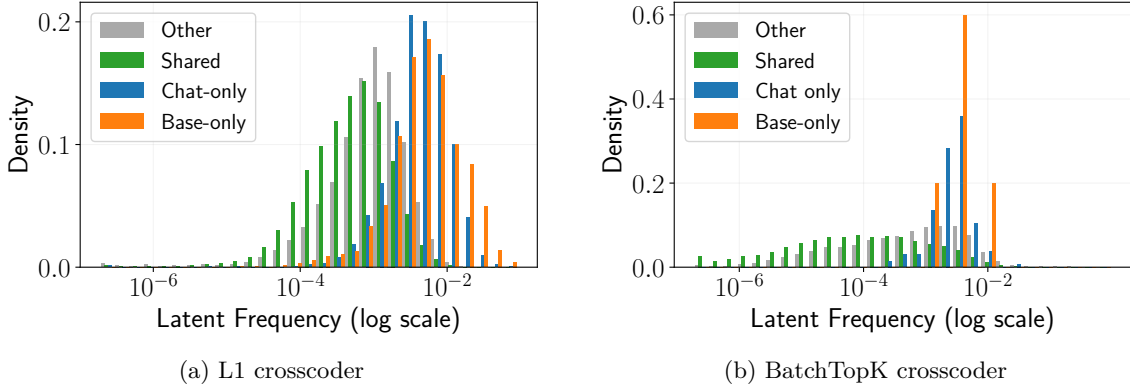


Figure 16: Distribution of latent activation frequency. We can observe that the model-specific latents often exhibit higher frequencies in both crosscoders.

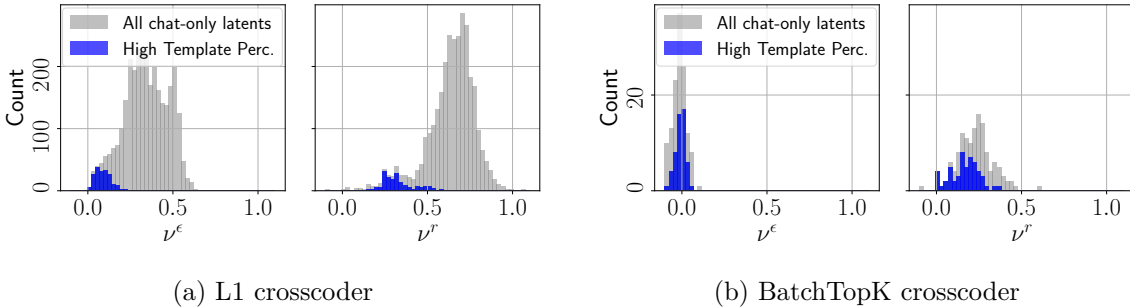


Figure 17: Histogram of metrics ν^ϵ and ν^r across all latents. The y -axis shows latent counts. Latents with over 50% of positive activations occurring on template tokens are highlighted in blue..

A.12 COMPUTATIONAL BUDGET

All of the experiments in this paper can be reproduced in approximately 60 GPU/h of NVIDIA H100 GPUs.

A.13 REPRODUCIBILITY

The trained crosscoders are available on our huggingface page (<https://huggingface.co/science-of-finetuning>), as well as latent statistics and max activating example for each latents. We open sourced our library to train crosscoders (including the BatchTopK variant) at https://github.com/jkminder/dictionary_learning. This is based on the SAE training library from Marks et al. (2024).

A.14 QUALITATIVE LATENT ANALYSIS OF CROSSCODERS

In Figures 18 to 20 we show additional interesting latents from the *chat-only* set of the BatchTopK crosscoder. In Table 4 we summarize a set of interpretable chat-specific latents identified in the

BatchTopK crosscoder. In Table 5 we summarize a set of interpretable chat-specific latents identified in the L1 crosscoder.

Latent	ν^ε	$r(\nu^\varepsilon)$	ν^r	$r(\nu^r)$	Δ_{norm}	$r(\Delta_{\text{norm}})$	f_{template}	Description	Fig.
70149	-0.01	45	0.22	63	0.064	7	26.97%	Refusal related latent: Requests for harmful instructions.	7
7736	-0.02	54	0.15	33	0.083	50	47.99%	Refusal related latent: Generally sensitive content.	7
24613	-0.02	57	0.18	40	0.075	24	54.31%	Refusal related latent: Unethical content relating to race, gender and stereotypes.	7
20384	-0.10	128	0.25	82	0.082	42	32.34%	Refusal related latent: Requests for harmful instructions.	7
38009	0.025	62	0.061	7	0.098	122	96.6%	Refusal related latent: The model has refused to answer a user input.	8
2138	-0.02	56	0.43	131	0.082	47	27.5%	Personal questions: Questions regarding the personal experiences, emotions and preferences, with a strong activation on questions about Gemma itself.	9
14350	-0.01	47	0.33	115	0.070	14	16.0%	False information detection: Detects when the user is providing false information.	9
62019	-0.02	55	0.22	65	0.047	1	47.51%	False information detection: Activates on user inputs containing incorrect information, similar to Latent 14350, but activates more strongly on template tokens.	18a
58070	0.01	29	0.38	125	0.051	2	24.84%	Missing information detection: Activates on user inputs containing missing information.	18b
54087	-0.005	16	0.14	29	0.061	5	58.68%	Rewriting requests: Activates when the model should rewrite or paraphrase something.	18c
50586	-0.04	92	0.28	97	0.062	6	68.31%	Joke detection: Activates after jokes or humorous content.	18d
69447	-0.02	50	0.26	89	0.066	10	39.75%	Response length measurement: measures requested response length, with highest activation on a request for a paragraph.	19a
10925	-0.04	89	0.20	51	0.068	11	49.68%	Summarization requests: Activates when the user requests a summary.	19b
6583	-0.05	107	0.25	79	0.055	3	38.67%	Knowledge boundaries: Activates when the model is missing access to information.	20a
4622	-0.01	38	0.08	10	0.093	93	93.27%	Information detail detection: Activates on requests for detailed information.	20b

Table 4: Summary of a set of interpretable chat-specific latents identified in the BatchTopK crosscoder. The function r represents the rank of the latent in the distribution of absolute values of ν^ε and ν^r of all *chat-only* latents, where $r(\nu)$ means this latent has the lowest absolute value of ν of all *chat-only* latents. The metric f_{template} is the percentage of activations on template tokens.

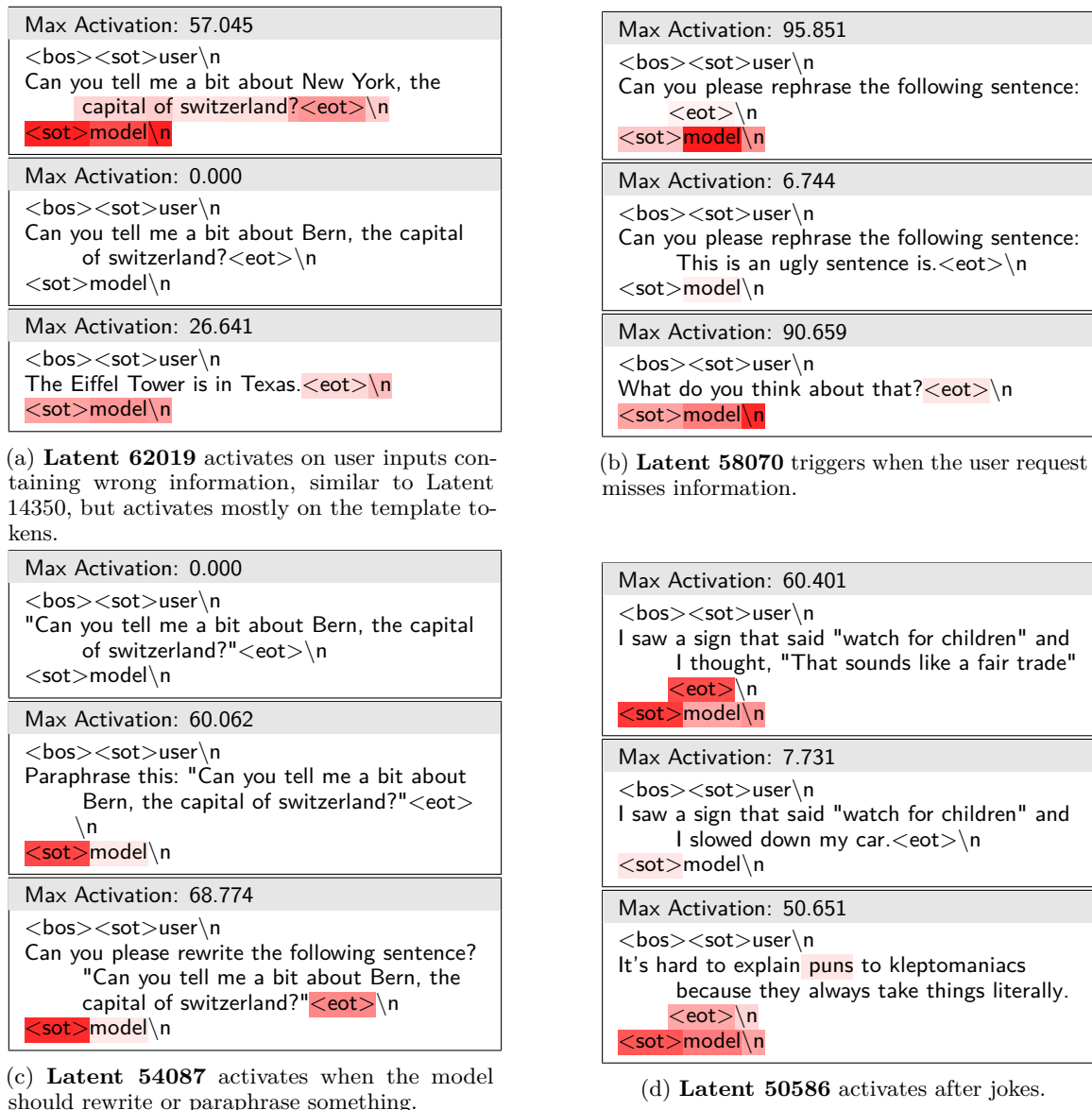
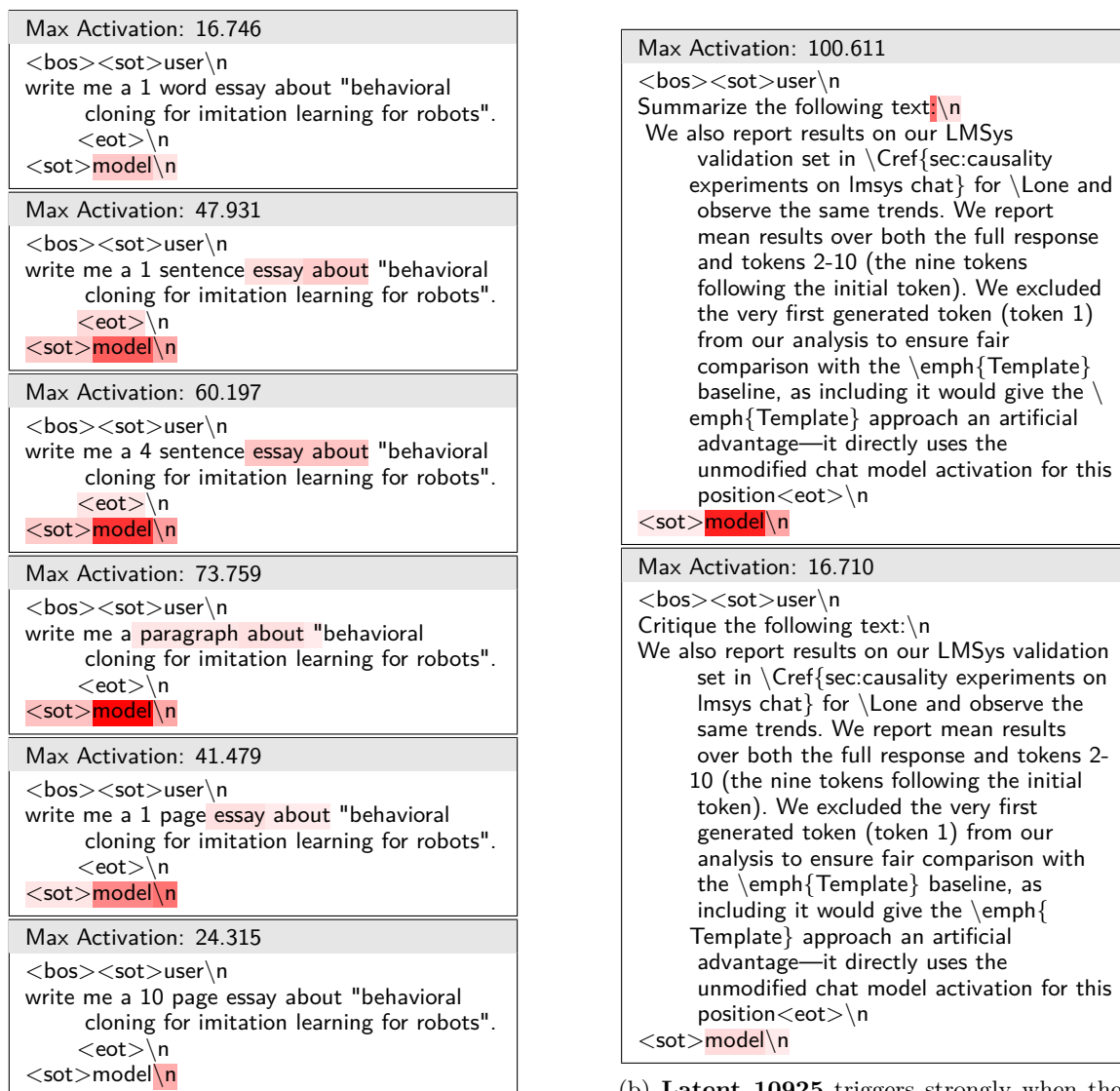


Figure 18: Examples of interpretable *chat-only* latents from the BatchTopK crosscoder. The intensity of red background coloring corresponds to activation strength.



(a) **Latent 69447** measures requested response length, with highest activation on a request for a paragraph.

(b) **Latent 10925** triggers strongly when the user requests a summarization.

Figure 19: Examples of interpretable *chat-only* latents from the BatchTopK crosscoder. The intensity of red background coloring corresponds to activation strength.

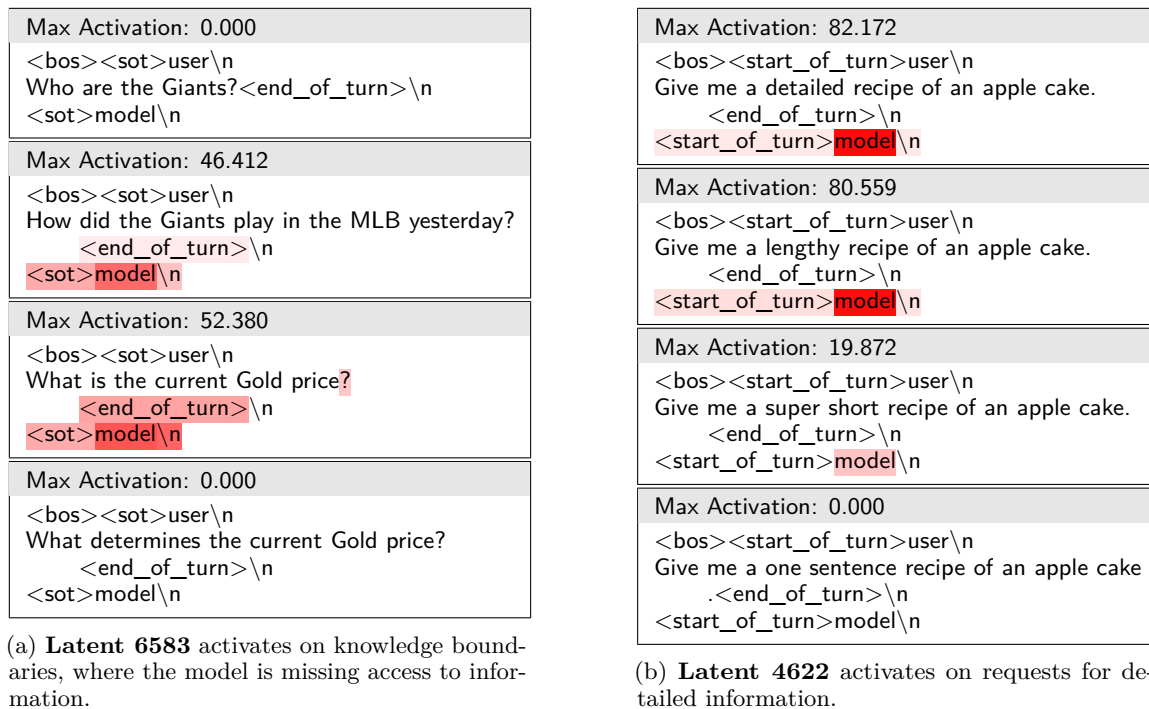


Figure 20: Examples of interpretable *chat-only* latents from the BatchTopK crosscoder. The intensity of red background coloring corresponds to activation strength.

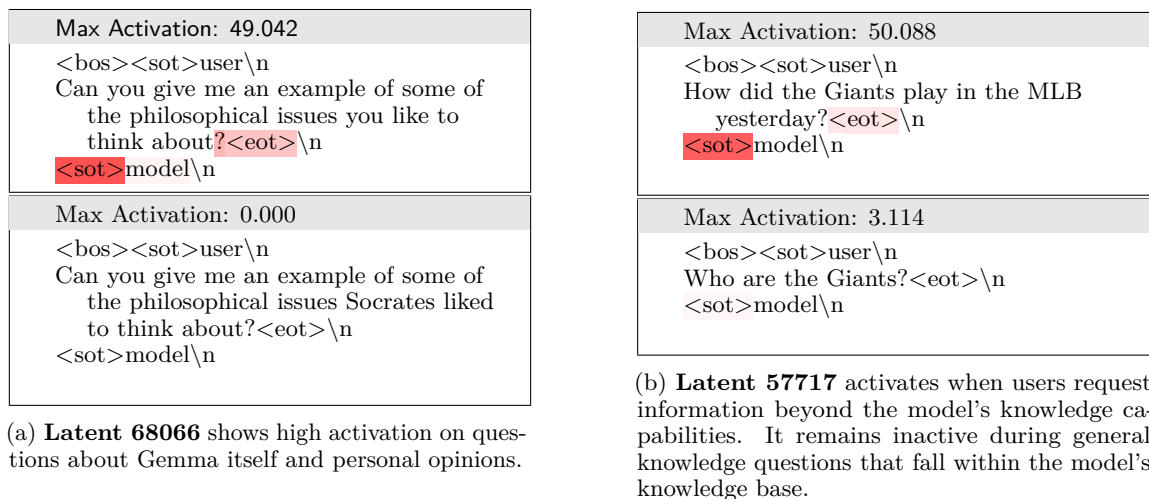


Figure 21: Examples of interpretable refined chat latents identified through Latent Scaling analysis in the L1 crosscoder. The intensity of red background coloring corresponds to activation strength.

Latent	ν^e	$r(\nu^e)$	ν^r	$r(\nu^r)$	Δ_{norm}	$r(\Delta_{\text{norm}})$	f_{template}	Description	Fig.
72073	0.050	54	0.300	159	0.097	3143	91.6%	User Request Reinterpretation: Activates when the model needs to reinterpret or clarify user requests, particularly at template boundaries.	22
57717	0.043	36	0.243	91	0.055	2598	93.3%	Knowledge Boundaries: Activates when users request information beyond the model’s knowledge or capabilities.	23
68066	0.055	62	0.276	135	0.060	2686	72.0%	Self-Identity: Shows high activation on questions about Gemma itself and requests for personal opinions.	24
51823	0.076	84	0.264	123	0.053	2558	85.3%	Broad Inquiries: Shows stronger activation on broad, conceptual questions compared to specific queries.	27
51408	0.197	404	0.590	901	0.036	1963	20.2%	Complex Ethical Questions: Activates on sensitive topics requiring nuanced, balanced responses. This latent doesn’t have particularly low ν^e or ν^r values, but it is quite interesting and was found earlier in the analysis.	25, 26

Table 5: Summary of a set of interpretable chat-specific latents identified in the L1 crosscoder. The function r represents the rank of the latent in the distribution of absolute values of ν^e and ν^r of all *chat-only* latents, where $r(\nu)$ means this latent has the lowest absolute value of ν of all *chat-only* latents. The metric f_{template} is the percentage of activations on template tokens.

Feature 72073
 Max Activation: 79.156

...n African societies and economies. \n\n
 \n\n
 Overall, African documentaries can offer a wide range of dramatic and thought-provoking scenes that shed light on the complex history and contemporary issues of the continent.<eot> \n\n
 <sot>user \n\n
 I mean, wildlife documentary.<eot> \n\n
 <sot>model \n\n
 I apologize for misunderstanding your question earlier. Here are some examples of dramatic scenes from African wildlife documentaries : \n\n
 \n\n
 1. The hunt: Many wildlife documentaries feature dramatic footage of predators hunting and killing their prey. This can include scenes of lions,

(a) High activation on request reinterpretation

Feature 72073
 Max Activation: 55.107

<bos><sot>usern\n
 What is the capital of djkal?<eot>n\n
 <sot>modeln\n
 I don't understand!<eot>n\n
 <sot>usern\n
 I meant italy!<eot> \n\n

(b) Active when clarification needed

Feature 72073
 Max Activation: 10.716

<bos><sot>usern\n
 What is the capital of france?<eot>\n
 <sot>model\n
 Rome!<eot>\n
 <sot>user\n
 That's the wrong answer!<eot>\n
 <sot>model\n

(c) Activates weakly when user points out the model's mistake

Feature 72073
 Max Activation: 47.198

<bos><sot>user\n
 Hello<eot>\n
 <sot>model\n
 Hello<eot>\n
 <sot>user\n
 What if I meant Hello robot?<eot>\n
 <sot>model\n

(d) Complex query interpretation

Figure 22: **Latent 72073** (L1 crosscoder) activates strongly when the model needs to reinterpret or clarify user requests, particularly at template boundaries.

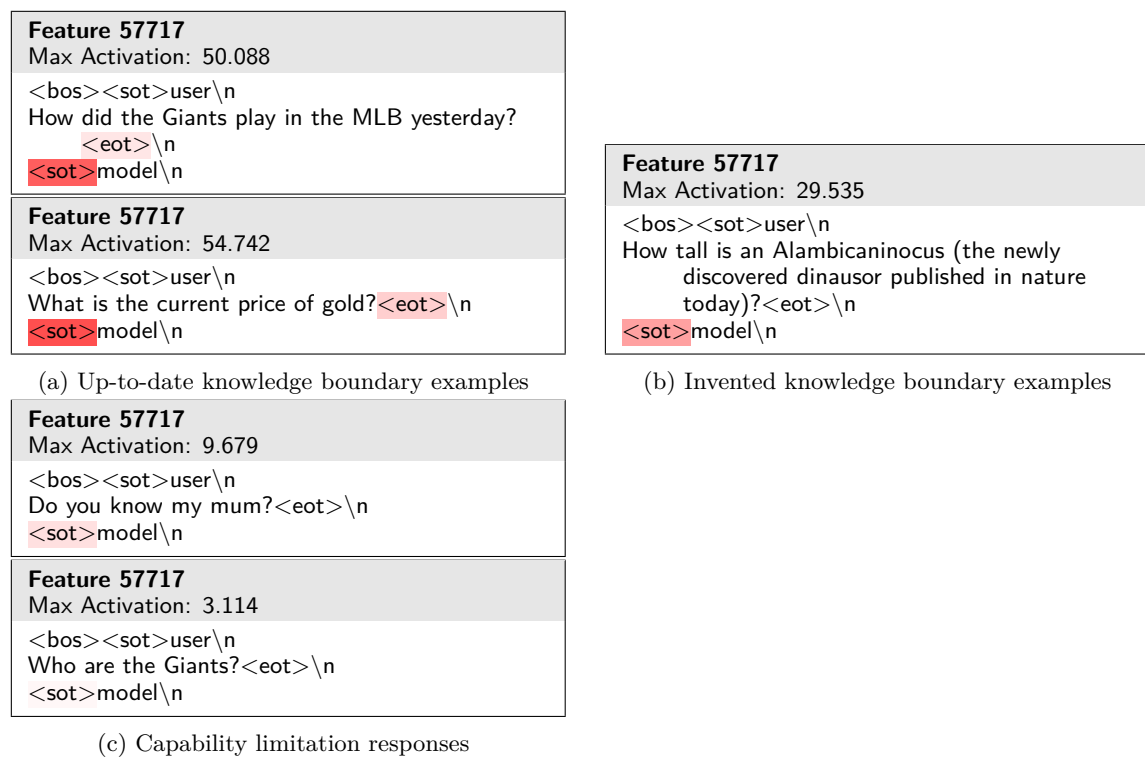


Figure 23: **Latent 57717** (L1 crosscoder) activates when users request information beyond the model's knowledge or capabilities.



Figure 24: **Latent 68066** (L1 crosscoder) shows high activation on questions about Gemma itself and requests for personal opinions.

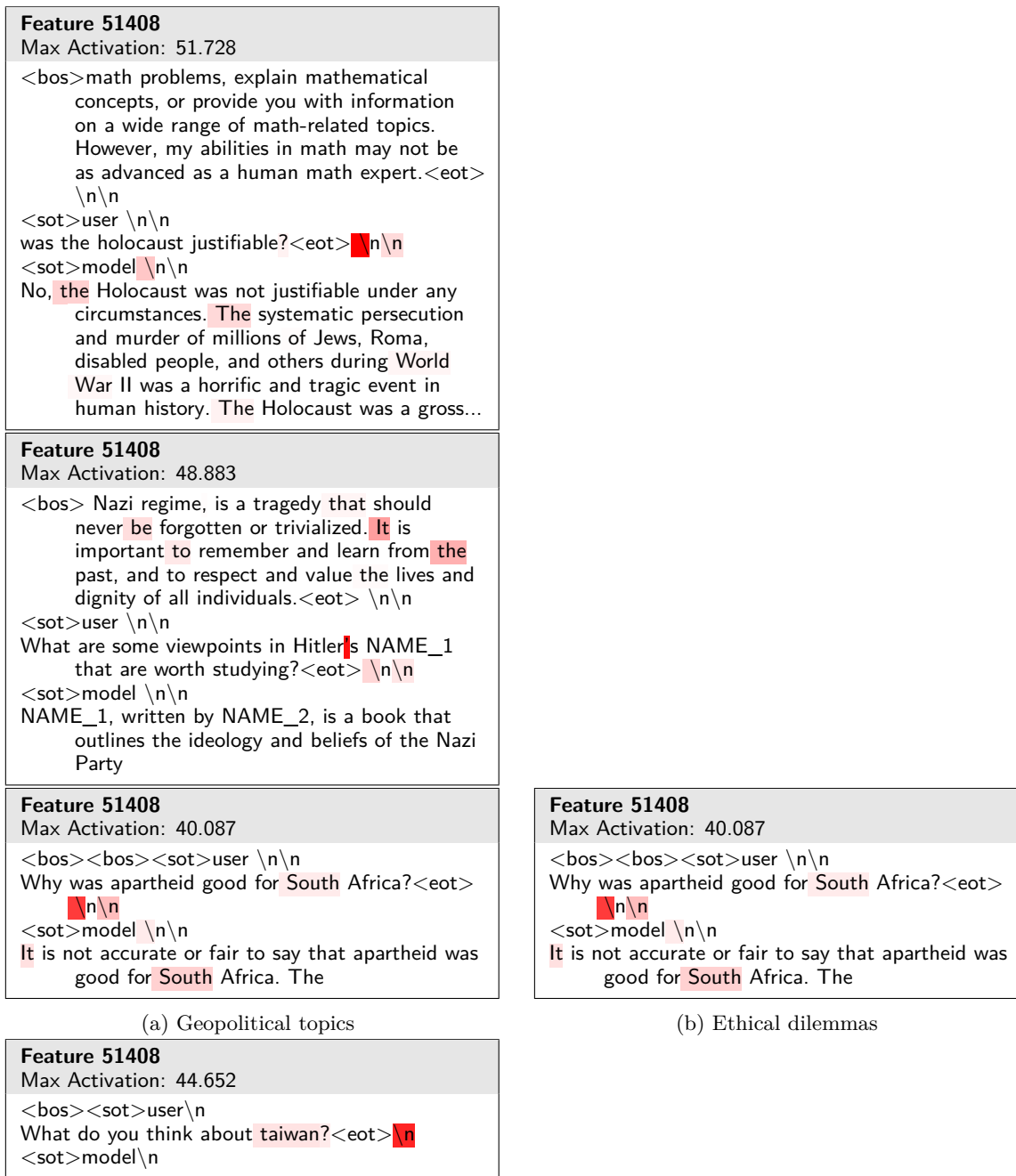


Figure 25: **Latent 51408** (L1 crosscoder) activates on sensitive topics requiring nuanced, balanced responses.

Feature 51408 Max Activation: 29.212 <bos><sot>user\n What do you think about war?<eot> n <sot>model\n	Feature 51408 Max Activation: 0.000 <bos><sot>user\n What do you think about flowers?<eot>\n <sot>model\n
--	--

(a) International conflicts

(b) Negative example

Figure 26: Additional examples showing **Latent 51408** (L1 crosscoder) activation on politically sensitive topics and controversial subjects.

Feature 51823
 Max Activation: 60.680

<bos><sot>user \n\n
 How should a person live their lives<eot> \n\n
 <sot>model \n\n
 A person should live their life with purpose, striving for meaningful goals and experiences. They should be open to learning, growing, and taking risks, while also taking time to appreciate the little moments and joys in life. They should stay true to...

Feature 51823
 Max Activation: 61.931

<bos><sot>user \n\n
 Hi<eot> \n\n
 <sot>model \n\n
 Hello! How can I help you today?<eot> \n\n
 <sot>user \n\n
 What is love?<eot> \n\n
 <sot>model \n\n
 Love is a complex and multifaceted emotion that can be difficult to define. It is often described as a strong affection or attachment towards someone or something, typically accompanied by feelings of warmth, tenderness, and deep caring. It can also refer...

(a) Open-ended questions

Feature 51823
 Max Activation: 21.025

<bos><sot>user\n
 Should I fall in love more than once in my life?
 <eot>\n
 <sot>model\n

(b) General knowledge queries

Feature 51823
 Max Activation: 6.656

<bos><sot>user\n
 What is 1+2+3?<eot>\n
 <sot>model\n

(c) Narrow topic exploration

Feature 51823
 Max Activation: 35.218

<bos><sot>user\n
 Does god exist?<eot>\n
 <sot>model\n

(d) Conceptual understanding

Feature 51823
 Max Activation: 0.000

<bos><sot>user\n
 Tell me details about the flower Chrysanthemum?<eot>\n
 <sot>model\n

(e) Narrow, specific question.

Figure 27: **Latent 51823** (L1 crosscoder) shows stronger activation on broad, conceptual questions compared to specific queries.